(12) INTERNATIONAL APPLICATION PUBLISHED UNDER THE PATENT COOPERATION TREATY (PCT)

(19) World Intellectual Property Organization
International Bureau

(43) International Publication Date
19 September 2019 (19.09.2019)

WIPO | PCT

(10) International Publication Number
WO 2019/173891 A1

(51) International Patent Classification:
H01M 10/056 (2010.01) *H01M 10/0525* (2010.01)

(21) International Application Number:
PCT/CA2018/000163

(22) International Filing Date:
31 August 2018 (31.08.2018)

(25) Filing Language: English

(26) Publication Language: English

(30) Priority Data:

62/641,957	12 March 2018 (12.03.2018)	US
62/702,549	24 July 2018 (24.07.2018)	US
16/057,119	07 August 2018 (07.08.2018)	US

(71) Applicant: **TESLA MOTORS CANADA ULC** [CA/CA]; 1325 Lawrence Avenue E, North York, Ontario M3A 1C6 (CA).

(72) Inventors: **DAHN, Jeffery, Raymond**; 1958 Rosebank Avenue, Halifax, Nova Scotia B3H 4C7 (CA). **MA, Xiaowei**; 175 Transom Drive, Halifax, Nova Scotia B3M 4T6 (CA). **GLAZIER, Stephen, Laurence**; 104 Lyons Avenue, Halifax, Nova Scotia B3P 1H5 (CA). **YOUNG, Robert, Scott**; 2058 East River East Side Road, New Glasgow, Nova Scotia B0K 1B0 (CA).

(74) Agent: **GOWLING WLG (CANADA) LLP**; Attn: TISDALL, Grant, Suite 1600, 1 First Canadian Place, 100 King Street West, Toronto, Ontario M5X 1G5 (CA).

(81) Designated States *(unless otherwise indicated, for every kind of national protection available)*: AE, AG, AL, AM, AO, AT, AU, AZ, BA, BB, BG, BH, BN, BR, BW, BY, BZ, CA, CH, CL, CN, CO, CR, CU, CZ, DE, DJ, DK, DM, DO, DZ, EC, EE, EG, ES, FI, GB, GD, GE, GH, GM, GT, HN, HR, HU, ID, IL, IN, IR, IS, JO, JP, KE, KG, KH, KN, KP, KR, KW, KZ, LA, LC, LK, LR, LS, LU, LY, MA, MD, ME, MG, MK, MN, MW, MX, MY, MZ, NA, NG, NI, NO, NZ, OM, PA, PE, PG, PH, PL, PT, QA, RO, RS, RU, RW, SA, SC, SD, SE, SG, SK, SL, SM, ST, SV, SY, TH, TJ, TM, TN, TR, TT, TZ, UA, UG, US, UZ, VC, VN, ZA, ZM, ZW.

(84) Designated States *(unless otherwise indicated, for every kind of regional protection available)*: ARIPO (BW, GH, GM, KE, LR, LS, MW, MZ, NA, RW, SD, SL, ST, SZ, TZ, UG, ZM, ZW), Eurasian (AM, AZ, BY, KG, KZ, RU, TJ, TM), European (AL, AT, BE, BG, CH, CY, CZ, DE, DK, EE, ES, FI, FR, GB, GR, HR, HU, IE, IS, IT, LT, LU, LV, MC, MK, MT, NL, NO, PL, PT, RO, RS, SE, SI, SK, SM,

(54) Title: NOVEL BATTERY SYSTEMS BASED ON TWO-ADDITIVE ELECTROLYTE SYSTEMS INCLUDING 1,2,6-OXODITHIANE-2,2,6,6-TETRAOXIDE

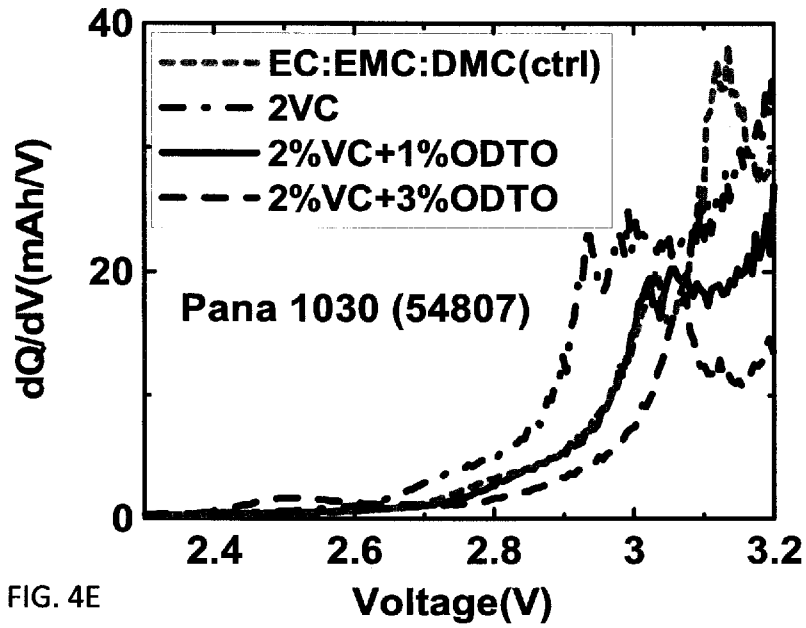

FIG. 4E

(57) Abstract: A nonaqueous electrolyte for a lithium ion battery comprising a lithium salt, a nonaqueous solvent, and an additive mixture comprising a first operative additive that is vinylene carbonate, $LiPO_2F_2$, fluoroethylene carbonate, or any combination of them, and a second operative additive that is 1,2,6-oxodithiane-2,2,6,6-tetraoxide.

WO 2019/173891 A1

[Continued on next page]

TR), OAPI (BF, BJ, CF, CG, CI, CM, GA, GN, GQ, GW, KM, ML, MR, NE, SN, TD, TG).

Published:

— *with international search report (Art. 21(3))*

NOVEL BATTERY SYSTEMS BASED ON TWO-ADDITIVE ELECTROLYTE SYSTEMS INCLUDING 1,2,6-OXODITHIANE-2,2,6,6-TETRAOXIDE

RELATED APPLICATION DATA

This application claims the benefit of priority of U.S. Provisional Application No. 62/641,957 filed March 12, 2018. This application also claims the benefit of priority of U.S. Provisional Application No. 62/702,549 filed July 24, 2018 the entirety of which is incorporated by reference herein to the extent permitted by law. This application also claims the benefit of priority of U.S. Patent Application No. 16/057,119 filed August 7, 2018, the entirety of which is incorporated by reference herein.

TECHNICAL FIELD

[0001] The present disclosure relates to rechargeable battery systems, and more specifically to the chemistry of such systems, including operative, electrolyte additives and electrodes, for improving the properties of the rechargeable lithium-ion-battery systems.

BACKGROUND

[0002] Rechargeable batteries are an integral component of energy-storage systems for electric vehicles and for grid storage (for example, for backup power during a power outage, as part of a microgrid, etc.). Depending on the application, the energy-storage systems require different properties. Tradeoffs in the chemistry of a battery system may need to be made to create a suitable system for a particular application. For example, in automobile applications—particularly those in an electric vehicle—the ability to charge and discharge quickly is an important property of the system. An electric vehicle owner may need to quickly accelerate in traffic, which requires the ability to quickly discharge the system. Further, fast charging and discharging places demands on the system, so the components of the system may also need to be chosen to provide sufficient lifetime under such operation conditions.

[0003] Electrolyte additives have been shown to be operative and increase the lifetime and performance of Li-ion-based batteries. For example, in J. C. Burns et al., *Journal of the Electrochemical Society,* 160, A1451 (2013), five proprietary, undisclosed electrolyte additives were shown to increase cycle life compared to an electrolyte system with no or only one additive. Other studies have focused on performance gains from electrolyte systems containing three or four additives as described in U.S. 2017/0025706. However, researchers typically do not understand the interaction between different additives that allow them to work together synergistically with the electrolyte and specific positive and negative electrodes. Thus, the composition of additive blends of certain systems is often based on trial and error and cannot be predicted beforehand.

[0004] Prior studies have not identified two-additive electrolyte systems that can be combined into a lithium-ion battery system to yield a robust system with sufficient properties for grid or automobile applications. As discussed in U.S. 2017/0025706, two-additive systems studied (for example, 2% VC + 1% allyl methanesulfonate and 2% PES + 1% TTSPi) typically performed worse than the three- and four-additive electrolyte systems. (*See, e.g.,* U.S. 2017/0025706 at Tables 1 and 2.) U.S. 2017/0025706 discloses that a third compound, often tris(-trimethly-silyl)-phosphate (TTSP) or tris(-trimethyl-silyl)-phosphite (TTSPi), was necessary in concentrations of between 0.25-3 wt% to produce a robust lithium-ion-battery system. (*See, e.g.,* U.S. 2017/0025706 at ¶72.) However, because additives can be expensive and difficult to include within Li-ion batteries on a manufacturing scale, more simple, yet effective electrolytes are needed, including those with fewer additives.

SUMMARY

[0005] This disclosure covers novel battery systems with fewer operative, electrolyte additives that may be used in different energy storage applications, for example, in vehicle and grid-storage. More specifically, this disclosure includes two-additive electrolyte systems that enhance performance and lifetime of Li-ion batteries, while reducing costs from other systems that rely on more additives. This disclosure also discloses effective positive electrodes and negative electrodes that work with the disclosed two-additive electrolyte systems to provide further systematic enhancements.

[0006] Operative additive electrolyte systems are disclosed including vinylene carbonate (VC) combined with 1,2,6-oxodithiane-2,2,6,6-tetraoxide (ODTO). ODTO has the following formula (I):

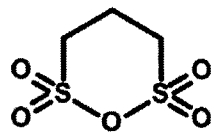

(I).

[0007] Also disclosed are fluoro ethylene carbonate (FEC) combined with ODTO and $LiPO_2F_2$ (called LFO here) combined with ODTO. Also disclosed are systems containing a combination of at least two of VC, LFO, and VC and ODTO.

[0008] Because VC and FEC provide similar improvements (and are believed to function similarly), a mixture of VC and FEC may be considered as only a single operative electrolyte. That is, another disclosed two-operative, additive electrolyte system includes a mixture of VC and FEC combined with ODTO. When used as part of a greater battery system (which includes the electrolyte, electrolyte solvent, positive electrode, and negative electrode), these two-operative, additive electrolyte systems produce desirable properties for energy storage applications, including in vehicle and grid applications. In addition, LFO acts effectively as a primary additive and can be combined with FEC and/or VC to make a additive system which can be further improved with LFO.

[0009] More specifically, lithium nickel manganese cobalt oxide (NMC) positive electrodes, graphite negative electrodes, a lithium salt dissolved in an organic or non-aqueous solvent, which may include methyl acetate (MA), and two additives can form a battery system with desirable properties for different applications. The electrolyte solvent may be the following solvents alone or in combination: ethylene carbonate (EC), ethyl methyl carbonate (EMC), methyl acetate, propylene carbonate, dimethyl carbonate, diethyl carbonate, another carbonate solvent (cyclic or acyclic), another organic solvent, and/or another non-aqueous solvent. Solvents are present in concentrations greater than the additives, typically greater than 6% by weight. The solvent may be combined with the disclosed two-additive pairs (such as VC with ODTO, FEC with ODTO, LFO with ODTO, a mixture of VC and FEC with ODTO, or another combination) to form a battery system with desirable properties for different applications. The positive electrode may be

coated with a material such as aluminum oxide (Al_2O_3), titanium dioxide (TiO_2), or another coating. Further, as a cost savings, the negative electrode may be formed from natural graphite, however depending on the pricing structure, in certain instances artificial graphite is cheaper than natural graphite.

[0010] The disclosure herein is supported by experimental data that shows the symbiotic nature of the two-additive electrolyte systems and selected electrodes. Exemplary battery systems include two additives (for example, FEC, LFO or VC, ODTO, a graphite negative electrode (either naturally occurring graphite or an artificial, synthetic graphite), an NMC positive electrode, a lithium electrolyte (formed from, for example, a lithium salt such as lithium hexafluorophosphate with chemical composition $LiPF_6$), and an organic or non-aqueous solvent. in further embodiments, the first additive is a combination of at least two of VC, LFO, and FEC.

[0011] An exemplary embodiment of this application is a nonaqueous electrolyte for a lithium ion battery comprising a lithium salt, a nonaqueous solvent, and an additive mixture comprising a first operative additive selected from vinylene carbonate, $LiPO_2F_2$ (LFO), fluoroethylene carbonate, or any combination of them, and a second operative additive of 1,2,6-oxodithiane-2,2,6,6-tetraoxide having the following formula (I):

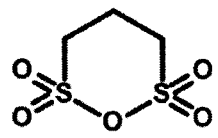

(I).

[0012] In another exemplary embodiment, a concentration of the first operative additive is in a range from 0.25 to 6% by weight.

[0013] In another exemplary embodiment, the concentration of the second operative additive is in a range from 0.25 to 5% by weight.

[0014] In another exemplary embodiment, the concentration of the first operative additive is 2% by weight (if it is VC or FEC) and 1% by weight (if it is LFO), and the concentration of the second operative additive is 1% by weight.

[0015] In another exemplary embodiment, the first operative additive is fluoroethylene carbonate.

[0016] In another exemplary embodiment, the first operative additive is vinylene carbonate.

[0017] In another exemplary embodiment, the first operative additive is $LiPO_2F_2$.

[0018] In another exemplary embodiment, the nonaqueous solvent is a carbonate solvent.

[0019] In another exemplary embodiment, the nonaqueous solvent is at least one selected from ethylene carbonate and ethyl methyl carbonate.

[0020] In another exemplary embodiment, the electrolyte further comprises a second nonaqueous solvent.

[0021] Another exemplary embodiment of this application is a lithium-ion battery comprising: a negative electrode; a positive electrode; and a nonaqueous electrolyte comprising lithium ions dissolved in a first nonaqueous solvent, and an additive mixture comprising: a first operative additive selected from fluoroethylene carbonate, $LiPO_2F_2$ and vinylene carbonate or any combination of them,; a second operative additive of 1,2,6-oxodithiane-2,2,6,6-tetraoxide having the following formula (I):

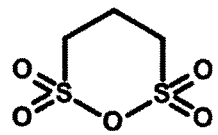

(I).

[0022] In another exemplary embodiment, a volume of gas produced in the lithium-ion battery is comparable with a volume of gas produced in a lithium-ion battery comprising only the first operative additive.

[0023] In another exemplary embodiment, the lithium-ion battery has 95% retention of initial capacity after 200 cycles between 3.0 V and 4.3 V at a charging rate of C/3 CCCV at 40°C.

[0024] In another exemplary embodiment, the lithium-ion battery has 95% retention of initial capacity after 300 cycles between 3.0 V and 4.3 V at a charging rate of C/3 CCCV at 40°C.

[0025] In another exemplary embodiment, the lithium-ion battery has 95% retention of initial capacity after 400 cycles between 3.0 V and 4.3 V at a charging rate of C/3 CCCV at 40°C.

[0026] In another exemplary embodiment, the lithium-ion battery has 95% retention of initial capacity after 500 cycles between 3.0 V and 4.3 V at a charging rate of C/3 CCCV at 40°C.

[0027] In another exemplary embodiment, the lithium-ion battery has 95% retention of initial capacity after 600 cycles between 3.0 V and 4.3 V at a charging rate of C/3 CCCV at 40°C.

[0028] In another exemplary embodiment, the lithium-ion battery has 95% retention of initial capacity after 700 cycles between 3.0 V and 4.3 V at a charging rate of C/3 CCCV at 40°C.

[0029] In another exemplary embodiment, the lithium-ion battery has 95% retention of initial capacity after 800 cycles between 3.0 V and 4.3 V at a charging rate of C/3 CCCV at 40°C.

[0030] In another exemplary embodiment, the lithium-ion battery has 95% retention of initial capacity after 900 cycles between 3.0 V and 4.3 V at a charging rate of C/3 CCCV at 40°C.

[0031] Another exemplary embodiment of this application is an electric vehicle with a rechargeable battery comprising: a drive motor; gear box; electronics; and a battery system as described herein.

BRIEF DESCRIPTION OF THE DRAWINGS

[0032] **FIG. 1** is a schematic diagram of a vehicle containing a battery storage system.

[0033] **FIG. 2** is a schematic diagram of an exemplary battery storage system.

[0034] **FIG. 3** is a schematic diagram of a lithium-ion, battery-cell system.

[0035] **FIGS. 4A-4E** illustrate the passivation impact of various electrolyte compositions in different types of cells.

[0036] **FIG. 4A** illustrates the passivation impact, by showing dQ/dV vs. V during the formation cycle of uncoated NMC532/artificial graphite cells containing electrolytes having ethylene carbonate (EC):ethyl methyl carbonate (EMC) (control), and EC:EMC with 2% VC, 1% ODTO, 3% ODTO, 5% ODTO, 2% VC + 1% ODTO, 2% FEC + 1% ODTO, and 1% LFO ($LiPO_2F_2$) + 1% ODTO.

[0037] **FIG. 4B** illustrates the passivation impact by showing dQ/dV vs. V during the formation cycle of coated NMC532/artificial graphite cells containing electrolytes having ethylene carbonate (EC):ethyl methyl carbonate (EMC) (control), and EC:EMC with 2% VC, 1% ODTO, 3% ODTO, 5% ODTO, 2% VC + 1% ODTO, 2% FEC + 1% ODTO, and 1% LFO + 1% ODTO.

[0038] **FIG. 4C** illustrates the passivation impact by showing dQ/dV vs. V during the formation cycle of Al_2O_3-coated NMC622/artificial graphite cells containing electrolytes having

1% ODTO, 3% ODTO, 5% ODTO, 2% VC + 1% ODTO, 2% FEC + 1% ODTO, 1% LFO + 1% ODTO, and 2% VC.

[0039] **FIG. 4D** illustrates the passivation impact by showing dQ/dV vs. V during the formation cycle of polycrystalline coating of aluminum, fluorine, and oxygen (AFO) coated NMC622/artificial graphite cells containing electrolytes having of ethylene carbonate (EC):ethyl methyl carbonate (EMC) (control), and EC:EMC with 1% ODTO, 3% ODTO, 5% ODTO, 2% VC + 1% ODTO, 2% FEC + 1% ODTO, 1% LFO + 1% ODTO, and 2% VC.

[0040] **FIG. 4E** illustrates the passivation impact by showing dQ/dV vs. V during the formation cycle of Panasonic 1030 cells containing electrolytes with 2% VC, 2% VC + 1% ODTO, and 2% VC + 3% ODTO.

[0041] **FIGS. 5A-5E** are the Electrochemical Impedance Spectroscopy (EIS) spectra of different types of cells with various electrolyte compositions.

[0042] **FIG. 5A** is the EIS spectra of different electrolyte systems comprising 1% ODTO, 3% ODTO, 5% ODTO, 2% VC + 1% ODTO, 2% FEC + 1% ODTO, 1% LFO + 1% ODTO, 2% VC, 2% FEC, and 1% LFO in a cell with an uncoated NMC532 positive electrode and an artificial graphite negative electrode.

[0043] **FIG. 5B** is the EIS spectra of different electrolyte systems comprising 1% ODTO, 3% ODTO, 5% ODTO, 2% VC + 1% ODTO, 2% FEC + 1% ODTO, 1% LFO + 1% ODTO, 1% LFO + 1% ODTO + 1% VC, 1% LFO + 1% ODTO + 1% FEC, 1% LFO + 1% ODTO + 1% TTSPi, 2% VC, 2% FEC, and 1% LFO in a cell with a coated NMC532 positive electrode and an artificial graphite negative electrode.

[0044] **FIG. 5C** is the EIS spectra of different electrolyte systems comprising 1% ODTO, 3% ODTO, 5% ODTO, 2% VC + 1% ODTO, 2% FEC + 1% ODTO, 1% LFO + 1% ODTO, 2% VC, and 2% FEC in a cell with an Al_2O_3-coated NMC622 positive electrode and an artificial graphite negative electrode.

[0045] **FIG. 5D** is the EIS spectra of different electrolyte systems comprising 1% ODTO, 3% ODTO, 5% ODTO, 2% VC + 1% ODTO, 2% FEC + 1% ODTO, 1% LFO + 1% ODTO, 2% VC, and 2% FEC in a cell with a AFO-coated NMC622 positive electrode and an artificial graphite negative electrode.

[0046] **FIG. 5E** is the EIS spectra of different electrolyte systems comprising 2% VC, 2% VC + 1% ODTO, 2% FEC + 3% ODTO in a Panasonic 1030 cell.

[0047] **FIGS. 6A-6E** illustrates the charge transfer resistance (R_{ct}) of different types of cells with various electrolyte compositions measured after the formation cycle.

[0048] **FIG. 6A** illustrates the R_{ct} of different electrolyte systems comprising 1% ODTO, 3% ODTO, 5% ODTO, 2% VC + 1% ODTO, 2% FEC + 1% ODTO, 1% LFO + 1% ODTO, 2% VC, 2% FEC, and 1% LFO in a cell with an uncoated NMC532 positive electrode and an artificial graphite negative electrode.

[0049] **FIG. 6B** illustrates the R_{ct} of different electrolyte systems comprising 1% ODTO, 3% ODTO, 5% ODTO, 2% VC + 1% ODTO, 2% FEC + 1% ODTO, 1% LFO + 1% ODTO, 2% VC, 2% FEC, and 1% LFO in a cell with a coated NMC532 positive electrode and an artificial graphite negative electrode.

[0050] **FIG. 6C** illustrates the R_{ct} of different electrolyte systems comprising 1% ODTO, 3% ODTO, 5% ODTO, 2% VC + 1% ODTO, 2% FEC + 1% ODTO, 1% LFO + 1% ODTO, 2% VC, and 2% FEC in a cell with an Al_2O_3-coated NMC622 positive electrode and an artificial graphite negative electrode.

[0051] **FIG. 6D** illustrates the R_{ct} of different electrolyte systems comprising 1% ODTO, 3% ODTO, 5% ODTO, 2% VC + 1% ODTO, 2% FEC + 1% ODTO, 1% LFO + 1% ODTO, 2% VC, and 2% FEC in a cell with a coated NMC622 positive electrode and an artificial graphite negative electrode.

[0052] **FIG. 6E** illustrates the R_{ct} of different electrolyte systems comprising2% VC, 2% VC + 1% ODTO, and 2% VC + 3% ODTO in a Panasonic 1030 cell with a coated NMC622 positive electrode and an artificial graphite negative electrode.

[0053] **FIGS. 7A-7E** summarizes the experimental data of the volume of formation gas generated during cell formation for different electrolyte systems.

[0054] **FIG. 7A** is a plot that summarizes experimental data of the volume of formation gas generated during cell formation for an electrolyte system comprising 1% ODTO, 3% ODTO, 5% ODTO, 2% VC + 1% ODTO, 2% FEC + 1% ODTO, 1% LFO + 1% ODTO, 2% VC, 2% FEC,

and 1% LFO in a cell with an uncoated NMC532 positive electrode and an artificial graphite negative electrode.

[0055] **FIG. 7B** is a plot that summarizes experimental data of the volume of formation gas generated during cell formation for an electrolyte system comprising 1% ODTO, 3% ODTO, 5% ODTO, 2% VC + 1% ODTO, 2% FEC + 1% ODTO, 1% LFO + 1% ODTO, 2% VC, 2% FEC, and 1% LFO in a cell with a coated NMC532 positive electrode and an artificial graphite negative electrode.

[0056] **FIG. 7C** is a plot that summarizes experimental data of the volume of formation gas generated during cell formation for an electrolyte system comprising 1% ODTO, 3% ODTO, 5% ODTO, 2% VC + 1% ODTO, 2% FEC + 1% ODTO, 1% LFO + 1% ODTO, 2% VC, and 2% FEC in a cell with an Al_2O_3-coated NMC622 positive electrode and an artificial graphite negative electrode.

[0057] **FIG. 7D** is a plot that summarizes experimental data of the volume of formation gas generated during cell formation for an electrolyte system comprising 1% ODTO, 3% ODTO, 5% ODTO, 2% VC + 1% ODTO, 2% FEC + 1% ODTO, 1% LFO + 1% ODTO, 2% VC, and 2% FEC in a cell with an AFO-coated NMC622 positive electrode and an artificial graphite negative electrode.

[0058] **FIG. 7E** is a plot that summarizes experimental data of the volume of formation gas generated during cell formation for an electrolyte system comprising 2% VC, 2% VC + 1% ODTO, and 2% VC + 3% ODTO in a Panasonic 1030 cell.

[0059] **FIGS. 8A-8B** illustrate the voltage versus time during high temperature storage for different NMC622/artificial graphite cells with various electrolyte systems.

[0060] **FIG. 8A** illustrates the voltage versus time during high temperature storage of electrolyte systems comprising 1% ODTO, 3% ODTO, 5% ODTO, 2% VC + 1% ODTO, 2% FEC + 1% ODTO, and 1% LFO + 1% ODTO in a cell with an Al_2O_3-coated NMC622 positive electrode and an artificial graphite negative electrode.

[0061] **FIG. 8B** illustrates the voltage versus time during high temperature storage of electrolyte systems comprising 1% ODTO, 3% ODTO, 5% ODTO, 2% VC + 1% ODTO, 2%

FEC + 1% ODTO, and 1% LFO + 1% ODTO in a cell with a coated NMC622 positive electrode and an artificial graphite negative electrode.

[0062] **FIG. 9** illustrates the parasitic heat flow in experiments involving various electrolyte additive systems in a Panasonic 1030 cell.

[0063] **FIGS. 10A-10W** illustrate experimental data collected during cycling experiments for various electrolyte systems, including discharge capacity, normalized discharge capacity (or fade rate), charge end point capacity, coulombic efficiency, and ΔV (difference between the average charge voltage and average discharge voltage).

[0064] **FIGS. 10A-10I** illustrate experimental data collected during cycling experiments for various additive electrolyte systems, including discharge capacity, normalized discharge capacity (or fade rate), charge end point capacity, coulombic efficiency, and ΔV (difference between the average charge voltage and average discharge voltage) using a coated NMC532 positive electrode and an artificial graphite negative electrode.

[0065] **FIGS. 10J-10K** illustrate experimental data collected during cycling experiments and ultra precision cycling experiments for various electrolyte systems, including discharge capacity, normalized discharge capacity (or fade rate), charge end point capacity, coulombic efficiency, and ΔV (difference between the average charge voltage and average discharge voltage) using uncoated NMC532 positive electrode and an artificial graphite negative electrode.

[0066] **FIGS. 10L-10R** illustrate experimental data collected during cycling experiments for various electrolyte systems, including discharge capacity, normalized discharge capacity (or fade rate), charge end point capacity, coulombic efficiency, and ΔV (difference between the average charge voltage and average discharge voltage) using Al_2O_3-coated and AFO-coated NMC622 positive electrode and an artificial graphite negative electrode.

[0067] **FIG. 10S** illustrates experimental data collected during cycling experiments for various electrolyte systems, including discharge capacity, normalized discharge capacity (or fade rate) and ΔV (difference between the average charge voltage and average discharge voltage) using Panasonic 1030 cells.

[0068] **FIG. 10T** illustrates experimental data collected during cycling experiments for various electrolyte systems, including discharge capacity, normalized discharge capacity (or fade

rate) and ΔV (difference between the average charge voltage and average discharge voltage) using Panasonic 1030 cells.

[0069] **FIG. 10U** illustrates experimental data collected during cycling experiments for various electrolyte systems, including discharge capacity, normalized discharge capacity (or fade rate), charge end point capacity, coulombic efficiency, and ΔV (difference between the average charge voltage and average discharge voltage) using Panasonic 1030 cells.

[0070] **FIG. 10V** illustrates experimental data collected during cycling experiments for various electrolyte systems, including discharge capacity, normalized discharge capacity (or fade rate) and ΔV (difference between the average charge voltage and average discharge voltage) using coated and uncoated NMC532 positive electrode and an artificial graphite negative electrode, and Al_2O_3-coated and AFO-coated NMC622 positive electrode and an artificial graphite negative electrode.

[0071] **FIG. 10W** illustrates experimental data collected during cycling experiments for various electrolyte systems, including discharge capacity, normalized discharge capacity (or fade rate) and ΔV (difference between the average charge voltage and average discharge voltage) using coated and uncoated NMC532 positive electrode and an artificial graphite negative electrode, and Al_2O_3-coated and AFO-coated NMC622 positive electrode and an artificial graphite negative electrode.

[0072] **FIG. 11** illustrates coulombic inefficiency per hour versus cycle number, fractional charge endpoint capacity slippage per hour versus cycle number, and fractional capacity fade per hour versus cycle number for electrolyte systems including 1% ODTO, 3% ODTO, 5% ODTO, 2% VC + 1% ODTO, 2% FEC + 1% ODTO, 1% LFO + 1% ODTO, 2%VC, and 2% FEC cycling between 3.0 V and 4.3 V, and using uncoated NMC532 positive electrode and an artificial graphite negative electrode.

[0073] **FIG. 12** illustrates coulombic inefficiency per hour versus cycle number, fractional charge endpoint capacity slippage per hour versus cycle number, and fractional capacity fade per hour versus cycle number for electrolyte systems including 1% ODTO, 3% ODTO, 5% ODTO, 2% VC + 1% ODTO, 2% FEC + 1% ODTO, 1% LFO + 1% ODTO, 2% VC, 2% FEC, and 1%

LFO cycling between 3.0 V and 4.3 V, and using coated NMC532 positive electrode and an artificial graphite negative electrode.

[0074] **FIG. 13** illustrates coulombic inefficiency per hour versus cycle number, fractional charge endpoint capacity slippage per hour versus cycle number, and fractional capacity fade per hour versus cycle number for electrolyte systems including 1% ODTO, 3% ODTO, 5% ODTO, 2% VC + 1% ODTO, 2% FEC + 1% ODTO, 1% LFO + 1% ODTO, 2% VC, and 2% FEC cycling between 3.0 V and 4.3 V, and using Al_2O_3-coated NMC622A positive electrode and an artificial graphite negative electrode.

[0075] **FIG. 14** illustrates coulombic inefficiency per hour versus cycle number, fractional charge endpoint capacity slippage per hour versus cycle number, and fractional capacity fade per hour versus cycle number for electrolyte systems including 1% ODTO, 3% ODTO, 5% ODTO, 2% VC + 1% ODTO, 2% FEC + 1% ODTO, 1% LFO + 1% ODTO, 2% VC, and 2% FEC cycling between 3.0 V and 4.3 V, and using AFO-coated NMC622B positive electrode and an artificial graphite negative electrode.

[0076] **FIG. 15** illustrates mean parasitic heat flow per cycle in experiments involving various electrolyte additive systems in a Panasonic 1030 cell.

[0077] **FIG. 16** illustrates the change in voltage over time and gas volume in experiments involving various electrolyte additive systems in a Panasonic 1030 cell.

[0078] **FIG. 17** illustrates the parasitic heat flow in experiments involving various electrolyte additive systems in a Panasonic 1030 cell.

DETAILED DESCRIPTION OF THE DISCLOSURE

[0079] **FIG. 1** illustrates the basic components of a battery powered electric vehicle (electric vehicle) 100. The electric vehicle 100 includes at least one drive motor (traction motor) 102A and/or 102B, at least one gear box 104A and/or 104B coupled to a corresponding drive motor 102A and/or 102B, battery cells 106 and electronics 108. Generally, the battery cells 106 provide electricity to power electronics of the electric vehicle 100 and to propel the electric vehicle 100 using the drive motor 102A and/or 102B. The electric vehicle 100 includes a large number of other components that are not described herein but known to one or ordinary skill. While the

construct of the electric vehicle 100 of **FIG. 1** is shown to have four wheels, differing electric vehicles may have fewer or more than four wheels. Further, differing types of electric vehicles 100 may incorporate the inventive concepts described herein, including motor cycles, aircraft, trucks, boats, train engines, among other types of vehicles. Certain parts created using embodiments of the present disclosure may be used in vehicle 100.

[0080] **FIG. 2** illustrates a schematic view of an exemplary energy storage system 200 showing various components. The energy storage system 200 typically includes a modular housing with at least a base 202 and four side walls 204 (only two shown in the figure). The module housing is generally electrically isolated from the housed battery cells 206. This may occur through physical separation, through an electrically insulating layer, through the choice of an insulating material as the module housing, any combination thereof, or another through another method. The base 202 may be an electrically insulating layer on top of a metal sheet or a nonconductive/electrically insulating material, such as polypropylene, polyurethane, polyvinyl chlorine, another plastic, a nonconductive composite, or an insulated carbon fiber. Side walls 204 may also contain an insulating layer or be formed out of a nonconductive or electrically insulating material, such as polypropylene, polyurethane, polyvinyl chlorine, another plastic, a nonconductive composite, or an insulated carbon fiber. One or more interconnect layers 230 may be positioned above the battery cells 206, with a top plate 210 positioned over the interconnect layer 230. The top plate 210 may either be a single plate or be formed from multiple plates.

[0081] Individual battery cells 106 and 206 often are lithium-ion battery cells, with an electrolyte containing lithium ions and positive and negative electrodes. **FIG. 3** illustrates a schematic of a lithium ion cell 300. Lithium ions 350 are dispersed throughout electrolyte 320, within container 360. Container 360 may be part of a battery cell. The lithium ions 350 migrate between positive electrode 330 and negative electrode 340. Separator 370 separates the negative electrode and positive electrode. Circuitry 310 connects the negative electrode and positive electrode.

[0082] New studies by the inventors have identified novel electrolyte and battery systems for use in grid and electric vehicle applications. These systems are based on two-additive electrolyte systems combined with solvents and electrodes, including vinylene carbonate (VC) combined with 1,2,6-oxodithiane-2,2,6,6-tetraoxide (ODTO), $LiPO_2F_2$ combined with ODTO and

fluoroethylene carbonate (FEC) combined with ODTO. These two-additive electrolyte systems are paired with a positive electrode made from lithium nickel manganese cobalt oxide with the composition $LNi_xMn_yCo_zO_2$ (abbreviated NMC generally or NMCxyz where the x, y, and z are the molar ratios of nickel, manganese and cobalt respectively. In certain embodiments, the positive electrode is formed from NMC111, NMC532, NMC811, or NMC622. In certain embodiments, NMC532 positive electrodes formed from single-crystal, micrometer-side particles, which resulted in an electrode with micrometer-size areas of continuous crystal lattice (or grains), have been shown to be particularly robust, in part because the materials and processing conditions result in larger grain sizes than using conventional materials and processing conditions.

[0083] Typical processing conditions lead to NMC electrodes with nanometer-sized particles packed into larger micrometer-sized agglomerates, creating grain boundaries on the nanometer scale. Grain boundaries are defects that tend to reduce desirable properties (for example, electrical properties), so it is typically desirable to reduce the number of grains and increase the grain size. Processing can create larger domains, on the micrometer size scale, thereby reducing the number of grain boundaries in the NMC electrodes, increasing electrical properties. The increase in properties is results in more robust battery systems. In certain embodiments, other NMC electrodes may be processed to create larger domain sizes (on the micrometer-size scale or larger), for example, NMC111, NMC811, NMC622, or another NMC compound to create more robust systems.

[0084] The positive electrode may be coated with a material such as aluminum oxide (Al_2O_3), titanium dioxide (TiO_2), or another coating. Coating the positive electrode is advantageous because it can help reduce interfacial phenomena at the positive electrode, such as parasitic reactions, or another phenomenon, that can deteriorate the cell containing the coated material. The negative electrode may be made from natural graphite, artificial graphite, or another material.

[0085] The electrolyte may be a lithium salt dissolved (such as $LiPF_6$) in a combination of organic or non-aqueous solvents, including ethylene carbonate, ethyl methyl carbonate, methyl acetate, propylene carbonate, dimethyl carbonate, diethyl carbonate, another carbonate solvent (cyclic or acyclic), another organic solvent, and/or another non-aqueous solvent. Solvents are

present in concentrations greater than the additives, typically greater than 5% by weight or 6% by weight. While the experimental data was generated using an electrolyte solvent that included EC:EMC:DMC 25:5:70 by volume (with or without methyl acetate (MA)), these solvents are merely exemplary of other carbonate solvents in particular and to other non-aqueous solvents. EC and EMC solvents were used in the experiments to control the systems tested in order to understand the effects of the additives and electrodes. Electrolyte systems may therefore may use other carbonate solvents and/or other non-carbonate solvents, including propylene carbonate, ethylene carbonate, dimethyl carbonate, ethyl methyl carbonate, diethyl carbonate, another carbonate solvent (cyclic or acyclic), another organic solvent, and/or another non-aqueous solvent. Solvents are present in concentrations greater than the additives, typically greater than 5% by weight or 6% by weight.

[0086] In the two-additive mixture FEC + ODTO, the concentration of FEC is preferentially between 0.5 to 6% by weight and the concentration of the ODTO is preferentially between 0.25 to 5% by weight. In the two-additive mixture VC + ODTO, the concentration of VC is preferentially between 0.5 to 6% by weight and the concentration of the ODTO is preferentially between 0.25 to 5% by weight. In the two-additive mixture LFO + ODTO, the concentration of LFO is preferentially between 0.5 to 1.5% by weight and the concentration of the ODTO is preferentially between 0.25 to 5% by weight.

[0087] Certain of these new battery systems may be used in energy-storage applications and also automobile application (including energy storage within an electric vehicle) in which charge and discharge speeds, and lifetime when charging and discharging quickly are important.

Pre-Experimental Setup

[0088] Although the battery systems themselves may be packaged differently according to the present disclosure, the experimental setup typically used machine made "sealed cells" to systematically evaluate the battery systems using a common setup, including the two-additive electrolyte systems and the specific materials for use the positive and negative electrodes. All percentages mentioned within this disclosure are weight percentages unless otherwise specified. A person of skill in the art will appreciate that the type of additive to be used and the concentration to be employed will depend on the characteristics which are most desirably

improved and the other components and design used in the lithium ion batteries to be made and will be apartment from this disclosure.

Sealed Battery Cells

[0089] The NMC/graphite sealed cells used in the experimental setup contained 1 M $LiPF_6$ in the solvent to which additives were added. The electrolyte consisted of 1 M $LiPF_6$ in 30% EC and 70% EMC. The concentration of the electrolyte components may be modified to include MA and/or DMC. To this electrolyte, the additive components were added at specified weight percentages.

[0090] The Panasonic 1030 sealed cells used in the experimental setup contained an electrolyte solvent that consisted of 1.2 M $LiPF_6$ added to EC, EMC and DMC in volume ratios of 25:5:70. To this electrolyte, the additive components were added at specified weight percentages.

[0091] The sealed NMC/graphite cells used a positive electrode made of NMC532 with micrometer-sized grains (sometimes referred to as single-crystal NMC532), and a negative electrode made of artificial graphite, unless otherwise specified. To test certain battery systems, other positive, including standard NMC532 (with smaller grains than the NMC with micrometer-sized grains) and NMC622, and negative electrodes (including natural graphite) were used.

[0092] Before electrolyte filling, the sealed cells were cut open below the heat seal and dried at 100°C under vacuum for 12 hours to remove any residual water. Then the cells were transferred immediately to an argon-filled glove box for filling and vacuum sealing and then were filled with electrolyte. After filling, cells were vacuum-sealed.

[0093] After sealing, the sealed cells were placed in a temperature box at 40.0 +/- 0.1° C and held at 1.5 V for 24 hours to allow for the completion of wetting. Then, sealed cells were subjected to the formation process. Unless specified otherwise, the formation process for NMC/graphite cells consisted of charging the sealed cells at 11 mA (C/20) to 4.2 V and discharging to 3.8 V. C/x indicates the that the time to charge or discharge the cell at the current selected is x hours when the cell has its initial capacity. For example, C/20 indicates that a charge or discharge would take 20 hours. After formation, cells were transferred and moved into

the glove box, cut open to release any generated gas and then vacuum sealed again and the appropriate experiments were performed.

[0094] The formation process for the Panasonic 1030 cells for the cycling and storage experiments consisted of charging the sealed cells at C/2 at 40°C for one hour; storing the cells at 60°C for 22 hours; charging the cells to 4.2 V and discharging to 3.8 V at C/2 at 40°C. After formation, cells were transferred and moved into the glove box, cut open to release any generated gas and then vacuum sealed again and the appropriate experiments were performed.

[0095] The formation process for the Panasonic 1030 cells for the charging profile and in-situ gas volume measurement experiments consisted of charging the sealed cells at C/20 at 40°C to 4.2 V and discharging to 3.8 V at C/20 at 40°C while they were connected to the in-situ gas measuring apparatus..

Passivation Impact

[0096] The passivation impact of various electrolyte compositions in different types of cells is illustrated in **FIGS. 4A-4E**. As seen from the data in **FIGS. 4A-4E**, ODTO shows similar passivation impact in five different types of cells. In the first and second cells (**FIGS. 4A-4B**), the passivation impact of ethylene carbonate (EC):ethyl methyl carbonate (EMC) (control), 2% VC, 1% ODTO, 3% ODTO, 5% ODTO, 2% VC + 1% ODTO, 2% FEC + 1% ODTO, and 1% LFO + 1% ODTO in a cell with an uncoated NMC532 positive electrode (**FIG. 4A**) and an artificial graphite negative electrode are compared and in a cell with a coated NMC532 positive electrode (**FIG. 4B**) and an artificial graphite electrode, is shown. In the third and fourth cells (**FIGS. 4C-4D**), the passivation impact of 2% VC, 1% LFO + 1% ODTO, 2% FEC + 1% ODTO, 2% VC + 1% ODTO, 1% ODTO, 3% ODTO, and 5% ODTO in a cell with Al_2O_3-coated NMC622/artificial graphite electrode (**FIG. 4C**) and a cell with an AFO-coated NMC622 electrode (**FIG. 4D**), is shown. And in the fifth cell (**FIG. 4E**), the passivation impact of EC:EMC:DMC, 2% VC, 2% VC + 1% ODTO, 2% VC + 3% ODTO, is shown. The peak at approximately 2.3 V corresponds to the reduction of ODTO when 1% ODTO is present (passivation peak). The effect of the 1% ODTO additive is independent of the type of positive electrode used, as demonstrated by a similar peak in **FIGS. 4C-4E**, which are directed to data for an Al_2O_3-coated NMC622 positive electrode, an AFO-coated NMC622 positive electrode, and an electrode as found in the Panasonic 1030 cell, respectively.

Cell Impedance

[0097] The two-additive electrolyte systems and novel battery systems disclosed herein have low cell impedance. Minimizing cell impedance is desirable since cell impedance decreases the energy efficiency of a cell. Conversely, low impedance leads to a higher possible charging rate and higher energy efficiency.

[0098] Cell impedance was measured using electrochemical impedance spectroscopy (EIS). Cells were charged or discharged to 3.80 V before they were moved to a 10.0 +/- 0.1 °C temperature box. AC impedance spectra were collected with ten points per decade from 100 kHz to 10 mHz with a signal amplitude of 10 mV at 10.0 +/- 0.1 °C. From the measured AC impedance, the charge transfer resistance (R_{ct}) was calculated and plotted.

[0099] In certain embodiments, two-additive electrolyte systems, the concentration of each additive about 0.25-6%, form part of the battery system. **FIGS. 5A-5E** show experimental data of cell charge transfer impedance experiments for two-additive electrolyte systems consisting of 1% ODTO, 3% ODTO, 5% ODTO, 2% VC + 1% ODTO, 2% FEC + 1% ODTO, 1% LFO + 1% ODTO, 2% VC, 2% FEC, and 1% LFO in a cell with an uncoated NMC532 positive electrode and an artificial graphite negative electrode (**FIG. 5A**); 1% ODTO, 3% ODTO, 5% ODTO, 2% VC + 1% ODTO, 2% FEC + 1% ODTO, 1% LFO + 1% ODTO, 1% LFO + 1% ODTO + 1% VC, 1% LFO + 1% ODTO + 1% FEC, 1% LFO + 1% ODTO + 1% TTSPi, 2% VC, 2% FEC, and 1% LFO in a cell with a coated NMC532 positive electrode and an artificial graphite negative electrode (**FIG. 5B**); 1% ODTO, 3% ODTO, 5% ODTO, 2% VC + 1% ODTO, 2% FEC + 1% ODTO, 1% LFO + 1% ODTO, 2% VC, and 2% FEC in a cell with an Al2O3-coated NMC622 positive electrode and an artificial graphite negative electrode (**FIG. 5C**); 1% ODTO, 3% ODTO, 5% ODTO, 2% VC + 1% ODTO, 2% FEC + 1% ODTO, 1% LFO + 1% ODTO, 2% VC, and 2% FEC in a cell with a AFO-coated NMC622 positive electrode and an artificial graphite negative electrode (**FIG. 5D**); and 2% VC, 2% VC + 1% ODTO, 2% FEC + 3% ODTO in a Panasonic 1030 cell (**FIG. 5E**). An artificial graphite negative electrode was used in each of these electrochemical cells.

[00100] The cell charge transfer impedance (R_{ct}) was also studied for these cells. As shown by the data in **FIGS. 6A-6E**, cell charge transfer impedance is reduced by 1% ODTO, alone or in combination of 2% FEC, 2% VC or 1% LFO, compared to electrolytes containing 3% ODTO or

5% ODTO. Therefore, these novel two-additive electrolyte systems do not sacrifice significant charge transfer impedance performance by including ODTO.

Gas Volume Measurements

[00101] The formation process is performed prior to cells being used in their intended application, such as grid storage or energy storage in an automobile, such as an electric vehicle. During formation, cells are subject to a precisely controlled charge and discharge cycle, which is intended to activate the electrodes and electrolyte for use in their intended application. During formation, gas is generated. If sufficient amounts of gas are generated (depending on the specific tolerances allowed by the cell and cell packaging), the gas may need to be released after the formation process and prior to application use. This typically requires the additional steps of breaking of a seal followed by a resealing. While these steps are common for many battery systems, it is desirable to remove them if possibly by choosing a system that produces less gas.

[00102] Gas volume experiments proceeded as follows: *Ex-situ* (static) gas measurements were used to measure gas evolution during formation and during cycling. The measurements were made using Archimedes' principle with cells suspended from a balance while submerged in liquid. The changes in the weight of the cell suspended in fluid, before and after testing are directly related to the volume changes by the change in the buoyant force. The change in mass of a cell, Δm, suspended in a fluid of density, ρ, is related to the change in cell volume, Δv, by $\Delta v = -\Delta m/\rho$. The gas generated during charge-discharge and during high potential hold periods was measured using the in-situ gas measuring device described by Aiken et al. (C. P. Aiken, J. Xia, David Yaohui Wang, D. A. Stevens, S. Trussler and J. R. Dahn, J. Electrochem. Soc. 2014 volume 161, A1548-A1554).

[00103] In certain embodiments, two-additive electrolyte systems, the concentration of each additive of about 0.25-6%, form part of the battery system. **FIGS. 7A-7E** shows the results of gas-generation experiments in two-additive electrolyte systems consisting of 1% ODTO, 3% ODTO, 5% ODTO, 2% VC + 1% ODTO, 2% FEC + 1% ODTO, 1% LFO + 1% ODTO, 2% VC, 2% FEC, and 1% LFO in a cell with an uncoated NMC532 positive electrode and an artificial graphite negative electrode(**FIG. 7A**); 1% ODTO, 3% ODTO, 5% ODTO, 2% VC + 1% ODTO, 2% FEC + 1% ODTO, 1% LFO + 1% ODTO, 2% VC, 2% FEC, and 1% LFO in a cell with a coated NMC532 positive electrode and an artificial graphite negative electrode(**FIG. 7B**); 1%

ODTO, 3% ODTO, 5% ODTO, 2% VC + 1% ODTO, 2% FEC + 1% ODTO, 1% LFO + 1% ODTO, 2% VC, and 2% FEC in a cell with an Al2O3-coated NMC622 positive electrode and an artificial graphite negative electrode (**FIG. 7C**); 1% ODTO, 3% ODTO, 5% ODTO, 2% VC + 1% ODTO, 2% FEC + 1% ODTO, 1% LFO + 1% ODTO, 2% VC, and 2% FEC in a cell with a coated NMC622 positive electrode and an artificial graphite negative electrode(**FIG. 7D**); 2% VC, 2% VC + 1% ODTO, and 2% VC + 3% ODTO in a Panasonic 1030 cell (**FIG. 7E**). An artificial graphite negative electrode was used in each of these electrochemical cells. In each of these cells, the amount of gas generated was measured according to the procedure described above. As shown in **FIGS. 7A-7E**, significant amounts of gas was produced in the cells with 1% ODTO or 1% LFO + 1% ODTO. However, gas production was significantly reduced in the cells with 2% VC + 1% ODTO and 2% FEC + 1% ODTO.

Storage Experiments

[00104] After formation, cells were discharged to 3 V and charged to 4.4 V twice with a current corresponding to C/10. Cells were then held 4.4 V for 24 h and afterwards transferred to a storage box at 60°C. The open-circuit voltage was recorded automatically every 6 h during a period of 500 h. Figure 8A and 8B show that cells incorporating 2VC + 1ODTO had the smallest amounts of self-discharge under these conditions.

Ultrahigh Precision Cycling

[00105] To study the effectiveness of the battery systems of the present disclosure, including the operative electrolyte additives and electrodes, ultrahigh precision cycling (UHPC) was performed. The standard UHPC procedure consisted of cycling cells between 3.0 and 4.3 V at 40°C using a current corresponding to C/20 for 15 cycles to produce the data. UPHC is employed to measure the coulombic efficiency, charge endpoint capacity slippage and other parameters to an accuracy of 30 ppm, in the case of the coulombic efficiency. Details of the UHPC procedure are described in T. M. Bond, J. C. Burns, D. A. Stevens, H. M. Dahn, and J. R. Dahn, *Journal of the Electrochemical Society*, 160, A521 (2013), which is incorporated herein in its entirety.

[00106] Metrics measured and/or determined from the UHPC measurements of particular interest include the following: coulombic efficiency, normalized coulombic inefficiency, normalized charge endpoint capacity slippage, normalized discharge capacity (or fade rate), and delta V. Coulombic efficiency is the discharge capacity (Q_d) divided by charge capacity (Q_c) of

the previous cycle. It tracks the parasitic reactions happening at the in the Li-ion cell and includes contributions from both the positive and negative electrodes. A higher CE value indicates less electrolyte degradation in the cell. Coulombic inefficiency per hour (CIE/h) is a normalized (per hour) coulombic inefficiency where the coulombic inefficiency is defined as 1-CE. It is calculated by taking 1-CE and dividing by the time of the cycle for which the CE was measured. Charge endpoint capacity motion (or slippage) tracks the parasitic reactions occurring at the positive electrode as well as the positive material mass loss, if any. Less motion is better and relates to less electrolyte oxidation. Normalized discharge capacity, or fade rate, is another important metric, with a lower fade rate desirable and normally indicative of a battery system with a longer lifetime. ΔV is calculated as the difference between the average charge voltage and average discharge voltage. ΔV change relates closely to polarization growth with lower ΔV change as cycling occurs is preferable. UHPC measurements are particularly appropriate for comparing electrolyte compositions because it allows for the tracking of metrics with a higher accuracy and precision and allows for the evaluation of various degradation mechanisms in a relatively rapid fashion.

[00107] Here, UHPC experiments were performed using 1% ODTO, 3% ODTO, 5% ODTO, 1% ODTO + 2% VC, 1% ODTO + 2% FEC, 1% ODTO + 1% LFO, 2%VC, 2% FEC, 2% VC, 20% MA + 2%VC, 20% MA + 2%VC + 1% ODTO, and 1% LFO. The material of the positive electrodes of the five different cells studied included uncoated (**FIG. 11**) and coated NMC 532 (**FIG. 12**) and Al_2O_3-coated NMC 622 (**FIG. 13**) and AFO-coated NMC622 (**FIG. 14**), and Panasonic 1030 cells. Raw data is shown in **FIGS. 10D** and **10E** for the coated NMC532 cells. Raw data is shown in **FIGS. 10J** and **10K** for uncoated NMC532 cells. Raw data is shown in **FIGS. 10O** and **10P** for Al_2O_3-coated NMC622 cells. Raw data is shown for AFO-coated NMC622 cells in **FIGS. 10Q** and **10R**. Raw data is shown for Panasonic 1030 cells in **FIG. 10U**.

[00108] In certain embodiments, two-additive electrolyte systems, the concentration of each additive of about 0.25-6%, form part of the battery system. The battery systems may also include positive electrodes made from NMC111, NMC532, NMC811, NMC622, or another NMC composition (NMCxyz). In certain embodiments, positive electrodes made from NMC532 with micrometer-scale grains have been shown to be particularly robust, in part because processing conditions created larger the grain sizes than typically processing conditions create.

[00109] Typical processing conditions lead to NMC electrodes with nanometer-sized particles packed into larger micrometer-sized agglomerates, creating grain boundaries on the nanometer scale. Grain boundaries are defects that tend to reduce desirable properties (for example, electrical properties), so it is typically desirable to reduce the number of grains and increase the grain size. Current processing can create larger domains, on the micrometer size scale, thereby reducing the number of grain boundaries in the NMC electrodes, increasing electrical properties. The increase in properties is results in more robust battery systems. In certain embodiments, other NMC electrodes may be processed to create larger domain sizes (on the micrometer-size scale or larger), for example, NMC111, NMC811, NMC622, or another NMC compound to create more robust systems.

Long Term Cycling

[00110] Lifetime of a battery system is an important property of a battery system. Charging and discharging rates can affect lifetime. Long term cycling experiments help determine how resilient battery systems are over time under anticipated operation conditions. It is important to select battery systems that have sufficient lifetimes for the desired application.

[00111] Embodiments of the present disclosure exhibit desirable long term cycling for different applications, including grid and vehicle storage. Specifically, two-additive electrolyte systems of VC + ODTO, LFO + ODTO, and FEC + ODTO are particularly relevant for automobile applications (especially energy storage within an electric vehicle) in which charging and discharging rates are typically higher than for grid-storage applications.

[00112] In the long-term-cycling experiments, single-crystal NMC532 and NMC 622 were typically used as the positive electrode (unless otherwise specified) and artificial graphite was used as the negative electrode (unless otherwise specified), as well as Panasonic 1030 cells. Before the long term cycling experiments, sealed cells were subjected to the formation processes as described above for each cell type. After formation, cells were cycled on a Neware charging systems.

[00113] In some experiments, cells were housed in a temperature controlled box at 40°C +/- 0.2°C. The cells were cycled between 3.0 V and the top of charge (4.2 V or 4.3 V) with a current of C/3 (half cycle of 3h), and a constant voltage step at the top of charge until the current dropped below C/20. Every 50 cycles, cells underwent one full cycle at C/20. Results from such

experiments for coated NMC532 are shown in **FIGS. 10A, 10B, 10C, 10V(b),** and **10W(b)** for uncoated NMC532 are shown in **FIGS. 10V(a) and 10W(a),** for Al_2O_3-coated coated NMC622 at **FIGS. 10L, 10V(c),** and **10W(c)**, for AFO-coated NMC622 at **FIGS. 10M, 10N, 10V(d), 10W(d)** and for Panasonic 1030 at **FIG. 10T(b)**.

[00114] In some experiments, cells were housed in a temperature controlled box at 55°C +/- 0.2°C. The cells were cycled between 3.0 V and the top of charge (4.2 V or 4.3 V) with a current of C/3 (half cycle of 3h), and a constant voltage step at the top of charge until the current dropped below C/20. Every 50 cycles, cells underwent one full cycle at C/20. Results from such experiments for coated NMC532 are shown in **FIGS. 10F** and **10G**, and for Panasonic 1030 at **FIG. 10S and 10T(c)**.

[00115] In some experiments, cells were housed in a temperature controlled box at 20°C +/- 0.2°C. The cells were cycled between 3.0 V and the top of charge (4.2 V or 4.3 V) with a current of C/3 (half cycle of 3h), and a constant voltage step at the top of charge until the current dropped below C/20. Every 50 cycles, cells underwent one full cycle at C/20. Results from such experiments for coated NMC532 are shown in **FIG. 10H**, and for Panasonic 1030 at **FIG. 10T(a)**.

[00116] In some experiments, cells were housed in a temperature controlled box at 20°C +/- 0.2°C. The cells were cycled between 3.0 V and the top of charge (4.2 V or 4.3 V) with a current of 1C (a charge takes one hour, and a discharge takes one hour), and a constant voltage step at the top of charge until the current dropped below C/20. Every 50 cycles, cells underwent one full cycle at C/20. Results from such experiments for coated NMC532 are shown in **FIG. 10I**.

[00117] The experimental data shows that the two-additive electrolyte systems (ODTO + FEC, ODTO + LFO, and DTD + VC) experience less capacity loss when cycling to 4.2 or 4.3 V and also lower polarization growth compared to the single additive electrolyte systems of VC or FEC, and the cycling is similar to 2% VC + 1% DTD and 1% LFO + 2FEC.

[00118] Additional studies were conducted with the Panasonic 1030 cells, including studies of the mean parasitic heat flow per cycle (**FIGS. 15, 17,** and **9**), and assessment of in-situ gas during charge-hold shown in **FIG. 16**.

[00119] Gas volume experiments proceeded as follows: *Ex-situ* (static) gas measurements were used to measure gas evolution during formation and during cycling. The measurements were made using Archimedes' principle with cells suspended from a balance while submerged in liquid. The changes in the weight of the cell suspended in fluid, before and after testing are directly related to the volume changes by the change in the buoyant force. The change in mass of a cell, Δm, suspended in a fluid of density, ρ, is related to the change in cell volume, Δv, by $\Delta v = -\Delta m/\rho$. The gas generated during charge-discharge and during high potential hold periods was measured using the in-situ gas measuring device described by Aiken et al. (C. P. Aiken, J. Xia, David Yaohui Wang, D. A. Stevens, S. Trussler and J. R. Dahn, J. Electrochem. Soc. 2014 volume 161, A1548-A1554).

[00120] The results in **FIG. 16** showed that ODTO is beneficial in suppressing gas at high voltage without or with 20%MA during charge/hold.

Microcalorimetry Measurements

[00121] Microcalorimetry measures heat flow to the cell during operation. The heat flow to the cell is a combination of three different effects: (1) ohmic heating, (2) entropy changes due to Li intercalating in the electrodes, and (3) parasitic reactions (electrolyte, including additive, degradation at either electrode). Because the test cells contain the same physical design, different only in the electrolyte, the difference in heat flow is primarily due to the differences in parasitic heat flow. Nevertheless, the parasitic heat flow can be extracted from the total heat flow using the procedures developed by Downie et al. (*Journal of the Electrochemical Society*, 161, A1782-A1787 (2014)) and by Glazier et al. (*Journal of the Electrochemical Society*, 164 (4) A567-A573 (2017)). Both of these references are incorporated herein in their entirety. Cells that have lower parasitic heat flow during cycling have better lifetimes. The voltage dependence of the parasitic reaction rate may be observed by plotting the measured parasitic heat flow as a function of cell voltage.

[00122] Microcalorimetry Measurement Procedure: Two cells of each electrolyte were connected to a Maccor charger and inserted into a TAMIII Microcalorimeter (TA Instruments, stability +/- 0.0001°C, accuracy +/- 1 μW, precision +/- 1 nW) at 40.0°C. The baseline drift over the course of the experiments did not exceed +/- 0.5 μW. All specifications and information regarding microcalorimetry calibration, cell connections, and operation procedures can be found

in previous literature. (For example, Downie et al, *ECS Electrochemical Letters 2*, A106-A109 (2013).) Cells were cycled four times at a C/20 rate between 3.0 V and 4.2 V to ensure well-formed, stable SEIs and were then charged between 4.0 V and different upper cut off limits at 3.7 mA (C/100) to investigate the performance and the parasitic heat flow in different voltage ranges. Each pair of cells yielded near identical performance, so only one set of heat flow data is presented for each electrolyte.

[00123] The 3.7 mA cycling protocol was:

1. Charge to 4.0 V, discharge to 3.9 V, repeat
2. Charge to 4.1 V, discharge to 3.9 V (repeat)
3. Charge to 4.2 V, discharge to 3.9 V (repeat)
6. Charge to 4.0 V, discharge to 3.9 V (repeat)

[00124] The experimental data shown in **FIGS. 15, 17** and **9** is for Panasonic 1030 cells were used which contained the electrolyte additives 2VC, 2VC+1ODTO, 2VC with 20% MA and 2VC+1ODTO with 20% MA. The utility of ODTO is observed when cells are tested between 3.9 and 4.2 V. In this situation, the parasitic heat flow is reduced suggesting Panasonic 1030 cells with 1%ODTO will have longer lifetimes when charged to 4.2 V (full state of charge). This is important to extend the lifetime of the battery pack in years or miles driven.

[00125] In certain embodiments, the positive electrode is formed from NMC111, NMC532, NMC822, NMC622, and/or NMCxyz. In particular, positive electrodes made from single-crystal NMC532 have been shown to be particularly robust, in part because the grain size of NMC532 is larger than the grain size of other standard NMC materials that are more polycrystalline, having smaller grain sizes.

[00126] The foregoing disclosure is not intended to limit the present disclosure to the precise forms or particular fields of use disclosed. As such, it is contemplated that various alternative embodiments and/or modifications to the present disclosure, whether explicitly described or implied herein, are possible in light of the disclosure. Having thus described embodiments of the present disclosure, a person of ordinary skill in the art will recognize that changes may be made in form and detail without departing from the scope of the present disclosure. Thus, the present disclosure is limited only by the claims. Reference to additives in the specification are generally to operative additives unless otherwise noted in the specification.

[00127] In the foregoing specification, the disclosure has been described with reference to specific embodiments. However, as one skilled in the art will appreciate, various embodiments disclosed herein can be modified or otherwise implemented in various other ways without departing from the spirit and scope of the disclosure. Accordingly, this description is to be considered as illustrative and is for the purpose of teaching those skilled in the art the manner of making and using various embodiments of the disclosed battery system. It is to be understood that the forms of disclosure herein shown and described are to be taken as representative embodiments. Equivalent elements, or materials may be substituted for those representatively illustrated and described herein. Moreover, certain features of the disclosure may be utilized independently of the use of other features, all as would be apparent to one skilled in the art after having the benefit of this description of the disclosure. Expressions such as "including", "comprising", "incorporating", "consisting of", "have", "is" used to describe and claim the present disclosure are intended to be construed in a non-exclusive manner, namely allowing for items, components or elements not explicitly described also to be present. Reference to the singular is also to be construed to relate to the plural. Reference to "about" or "approximately" is to be construed to mean plus or minus 10%. Similarly, reference to any percentage of an additive is construed to mean plus or minus 10%.

[00128] Further, various embodiments disclosed herein are to be taken in the illustrative and explanatory sense, and should in no way be construed as limiting of the present disclosure. All joinder references (*e.g.*, attached, affixed, coupled, connected, and the like) are only used to aid the reader's understanding of the present disclosure, and may not create limitations, particularly as to the position, orientation, or use of the systems and/or methods disclosed herein. Therefore, joinder references, if any, are to be construed broadly. Moreover, such joinder references do not necessarily infer that two elements are directly connected to each other.

[00129] Additionally, all numerical terms, such as, but not limited to, "first", "second", "third", "primary", "secondary", "main" or any other ordinary and/or numerical terms, should also be taken only as identifiers, to assist the reader's understanding of the various elements, embodiments, variations and/ or modifications of the present disclosure, and may not create any limitations, particularly as to the order, or preference, of any element, embodiment, variation and/or modification relative to, or over, another element, embodiment, variation and/or modification.

[00130] It will also be appreciated that one or more of the elements depicted in the drawings/figures can also be implemented in a more separated or integrated manner, or even removed or rendered as inoperable in certain cases, as is useful in accordance with a particular application.

CLAIMS

What is claimed is:

1. A nonaqueous electrolyte for a lithium ion battery comprising a lithium salt, a nonaqueous solvent, and an additive mixture comprising a first operative additive that is vinylene carbonate, $LiPO_2F_2$, fluoroethylene carbonate, or any combination of them, and a second operative additive that is 1,2,6-oxodithiane-2,2,6,6-tetraoxide having the following formula (I):

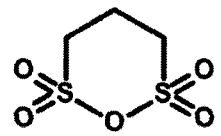

(I).

2. The nonaqueous electrolyte of claim 1, wherein a concentration of the first operative additive is in a range from 0.25 to 6% by weight.

3. The nonaqueous electrolyte of claim 1, wherein the concentration of the second operative additive is in a range from 0.25 to 5% by weight.

4. The nonaqueous electrolyte of claim 1, wherein the concentration of the first operative additive is at least 1% by weight, and the concentration of the second operative additive is at least 1% by weight.

5. The nonaqueous electrolyte of claim 4, wherein the first operative additive is fluoroethylene carbonate.

6. The nonaqueous electrolyte of claim 4, wherein the first operative additive is vinylene carbonate.

7. The nonaqueous electrolyte of claim 4, wherein the first operative additive is $LiPO_2F_2$

8. The nonaqueous electrolyte of claim 1, wherein the nonaqueous solvent is a carbonate solvent.

9. The nonaqueous electrolyte of claim 8, wherein the nonaqueous solvent is at least one selected from ethylene carbonate and ethyl methyl carbonate.

10. The nonaqueous electrolyte of claim 8, further comprising a second nonaqueous solvent.

11. A lithium-ion battery comprising:

a negative electrode;

a positive electrode; and

a nonaqueous electrolyte comprising lithium ions dissolved in a first nonaqueous solvent, and an additive mixture comprising:

a first operative additive that is fluoroethylene carbonate, $LiPO_2F_2$, vinylene carbonate, or any combination of them, and

a second operative additive that is 1,2,6-oxodithiane-2,2,6,6-tetraoxide having the following formula (I):

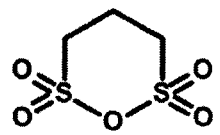

(I).

12. The lithium-ion battery of claim 11, wherein a concentration of the first operative additive is in a range from 0.25 to 6% by weight.

13. The lithium-ion battery of claim 11, wherein a concentration of the second operative additive is in a range from 0.25 to 5% by weight.

14. The lithium-ion battery of claim 11, wherein the concentration of the first operative additive is at least 1% by weight, and the concentration of the second operative additive is 1% by weight.

15. The lithium-ion battery of claim 14, wherein the first operative additive is fluoroethylene carbonate.

16. The lithium-ion battery of claim 14, wherein the first operative additive is vinylene carbonate.

17. The lithium-ion battery of claim 14, wherein the first operative additive is $LiPO_2F_2$.

18. The lithium-ion battery of claim 11, wherein the nonaqueous solvent is a carbonate solvent.

19. The lithium-ion battery of claim 18, wherein the nonaqueous solvent is selected from ethylene carbonate and ethyl methyl carbonate.

20. The lithium-ion battery of claim 18, further comprising a second nonaqueous solvent.

21. The lithium-ion battery of claim 14, wherein a volume of gas produced in the lithium-ion battery is comparable with a volume of gas produced in a lithium-ion battery comprising only the first operative additive.

22. The lithium-ion battery of claim 21, wherein the lithium-ion battery has at least 95% retention of initial capacity after 200 cycles between 3.0 V and 4.3 V at a charging rate of C/3 CCCV at 40°C.

23. The lithium-ion battery of claim 21, wherein the lithium-ion battery has at least 95% retention of initial capacity after 800 cycles between 3.0 V and 4.3 V at a charging rate of C/3 CCCV at 40°C.

24. An electric vehicle with a rechargeable battery comprising:
a drive motor;
gear box;
electronics; and
the lithium-ion battery of claim 11.

25. The electric vehicle of claim 24, wherein a concentration of the first operative additive is in a range from 0.25 to 6% by weight.

26. The electric vehicle of claim 24, wherein a concentration of the second operative additive is in a range from 0.25 to 5% by weight.

27. The electric vehicle of claim 24, wherein the concentration of the first operative additive is at least 1% by weight, and a concentration of the second operative additive is at least 1% by weight.

28. The electric vehicle of claim 27, wherein the first operative additive fluoroethylene carbonate.

29. The electric vehicle of claim 27, wherein the first operative additive is vinylene carbonate.

30. The electric vehicle of claim 27, wherein the first operative additive is $LiPO_2F_2$.

31. The electric vehicle of claim 24, wherein the nonaqueous solvent is a carbonate solvent.

32. The electric vehicle of claim 31, wherein the nonaqueous solvent is at least one selected from ethylene carbonate and ethyl methyl carbonate.

33. The electric vehicle of claim 32, wherein the lithium-ion battery further comprises a second nonaqueous solvent.

34. The electric vehicle of claim 24, wherein a volume of gas produced in the battery system is comparable with a volume of gas produced in a battery system comprising only the first operative additive.

35. The electric vehicle of claim 24, wherein the battery system has at least 95% retention of initial capacity after 200 cycles between 3.0 V and 4.3 V at a charging rate of C/3 CCCV at 40°C.

36. The electric vehicle of claim 31, wherein the battery system has at least 95% retention of initial capacity after 800 cycles between 3.0 V and 4.3 V at a charging rate of C/3 CCCV at 40°C.

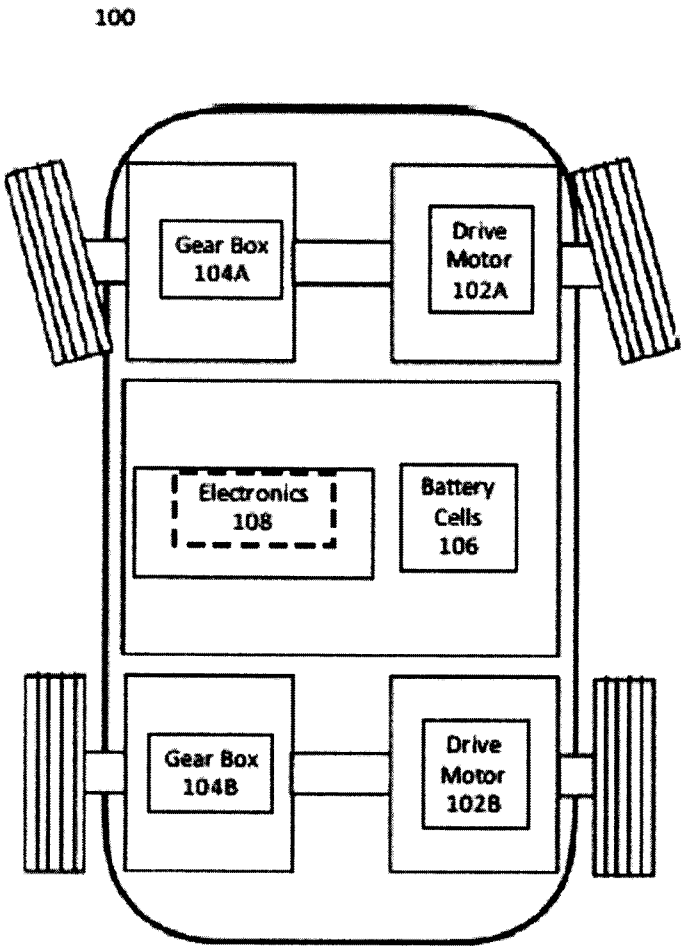
100
Gear Box
104A
Drive
Motor
102A
Electronics
108
Battery
Cells
106
Gear Box
104B
Drive
Motor
102B

FIG. 1

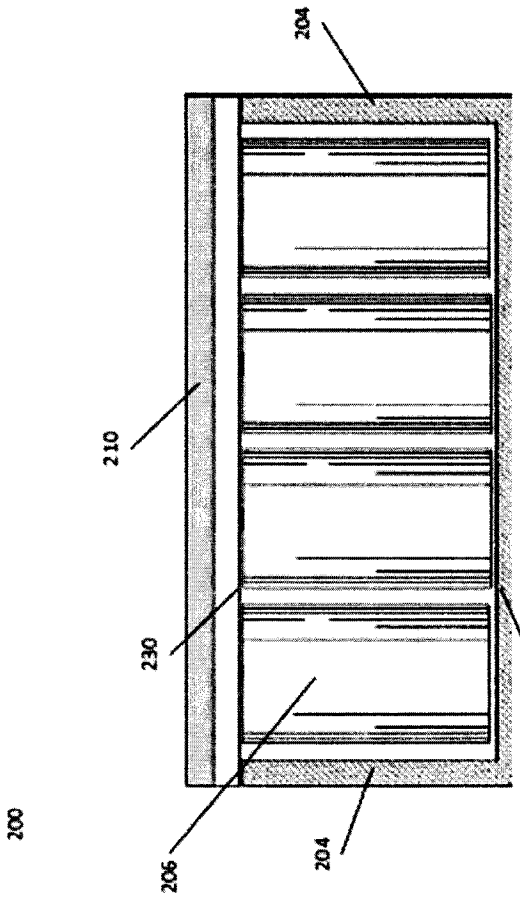

FIG. 2

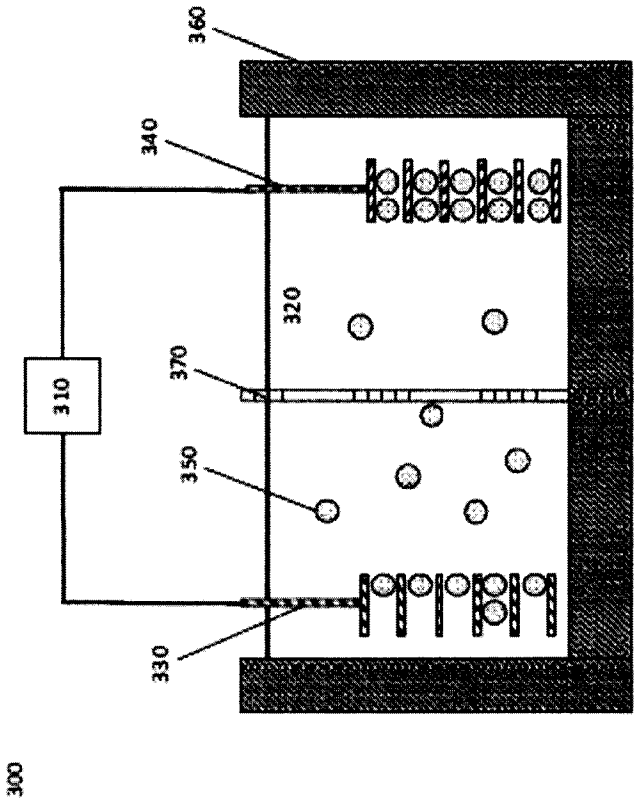

FIG. 3

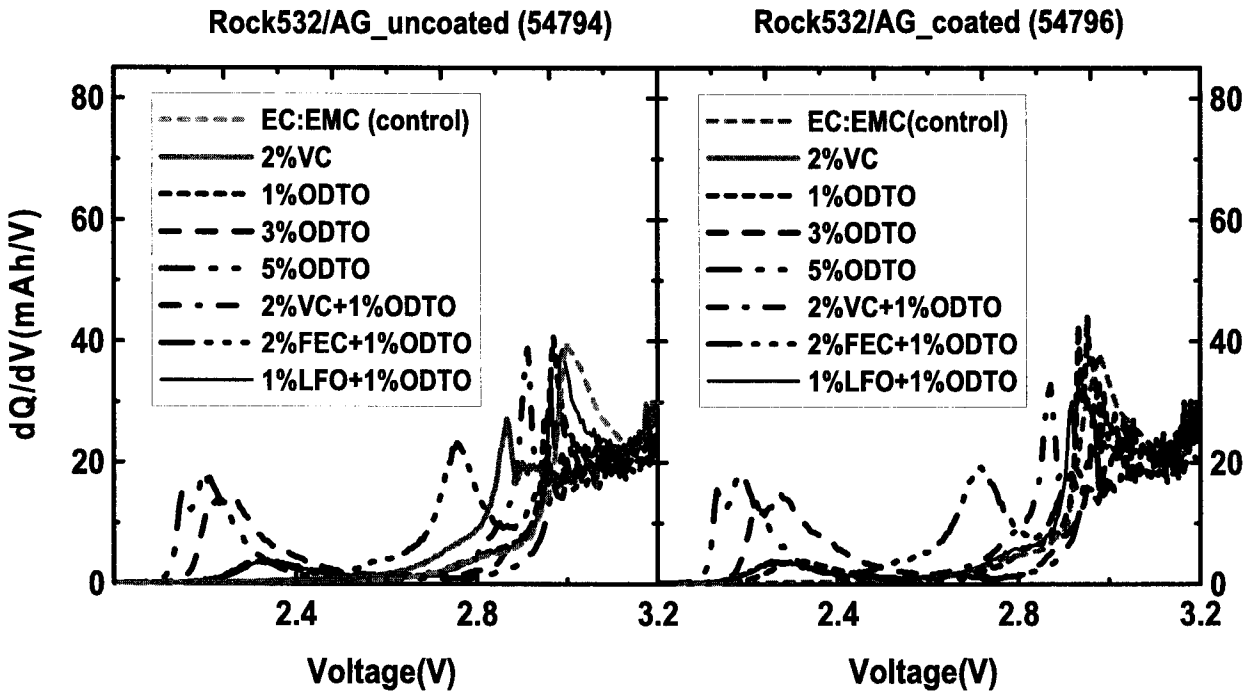
Rock532/AG_uncoated (54794)
Rock532/AG_coated (54796)
dQ/dV(mAh/V)
EC:EMC (control)
2%VC
1%ODTO
3%ODTO
5%ODTO
2%VC+1%ODTO
2%FEC+1%ODTO
1%LFO+1%ODTO
EC:EMC(control)
0
20
40
60
80
2.4
2.8
3.2
Voltage(V)

FIG. 4A

FIG. 4B

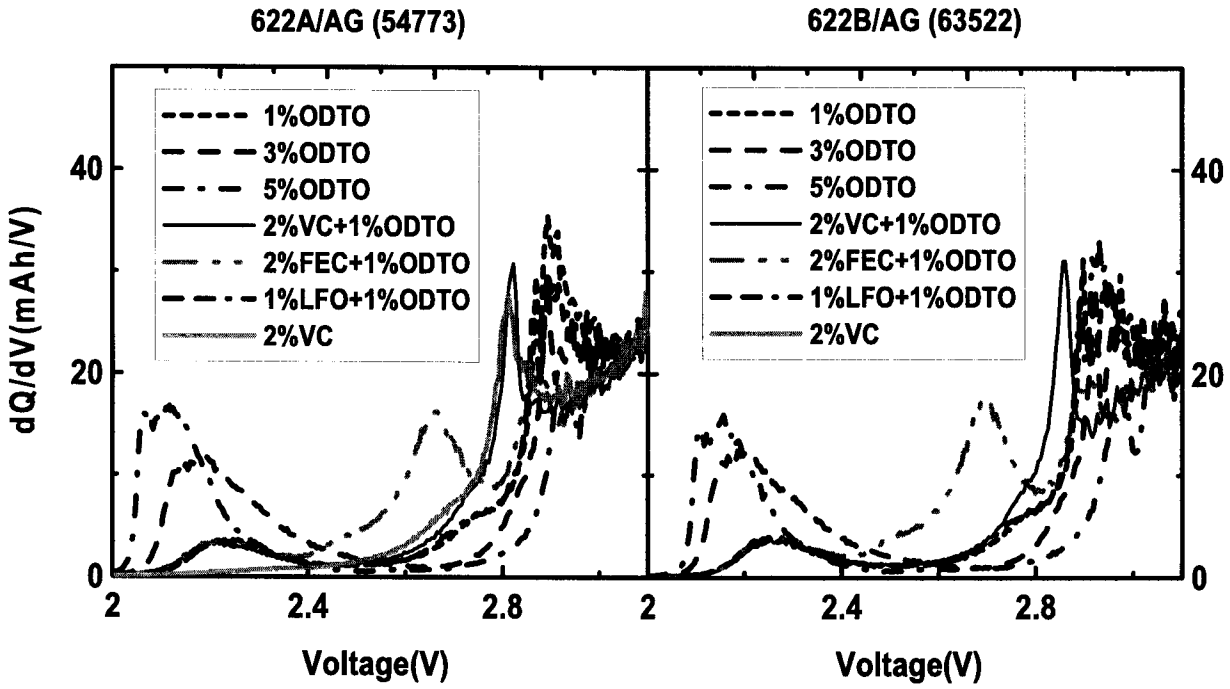
622A/AG (54773)
622B/AG (63522)
1%ODTO
3%ODTO
5%ODTO
2%VC+1%ODTO
2%FEC+1%ODTO
1%LFO+1%ODTO
2%VC
dQ/dV(mAh/V)
Voltage(V)
0
20
40
2
2.4
2.8

FIG. 4C

FIG. 4D

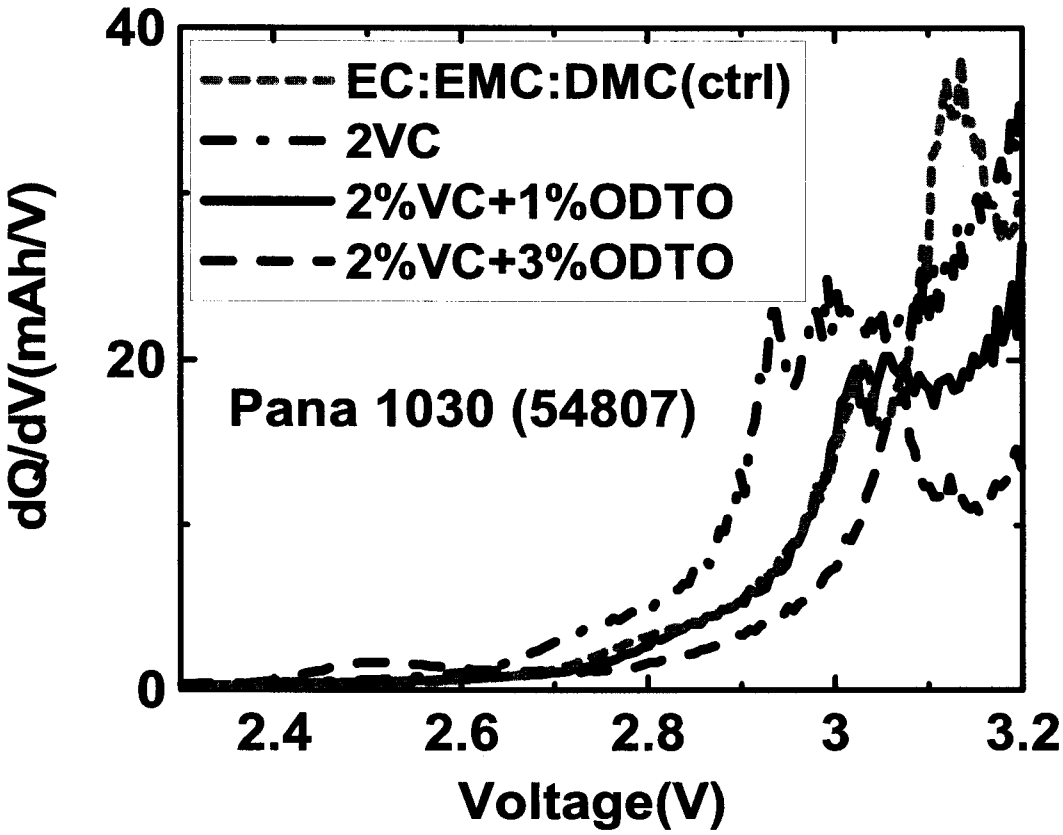
40
20
0
dQ/dV(mAh/V)
EC:EMC:DMC(ctrl)
2VC
2%VC+1%ODTO
2%VC+3%ODTO
Pana 1030 (54807)
2.4
2.6
2.8
3
3.2
Voltage(V)

FIG. 4E

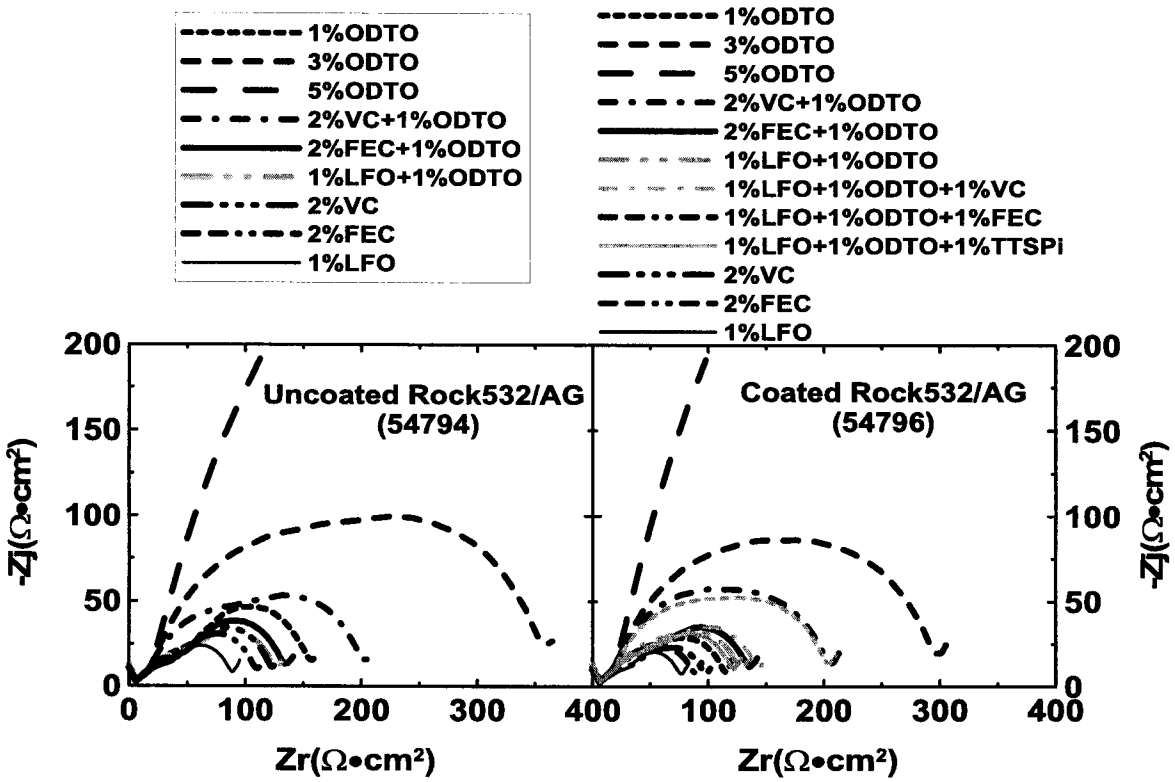
1%ODTO
3%ODTO
5%ODTO
2%VC+1%ODTO
2%FEC+1%ODTO
1%LFO+1%ODTO
2%VC
2%FEC
1%LFO
Uncoated Rock532/AG
(54794)
-Zj(Ω•cm²)
Zr(Ω•cm²)
0
50
100
150
200
0
100
200
300
400

FIG. 5A

1%ODTO
3%ODTO
5%ODTO
2%VC+1%ODTO
2%FEC+1%ODTO
1%LFO+1%ODTO
1%LFO+1%ODTO+1%VC
1%LFO+1%ODTO+1%FEC
1%LFO+1%ODTO+1%TTSPi
2%VC
2%FEC
1%LFO
Coated Rock532/AG
(54796)
-Zj(Ω•cm²)
Zr(Ω•cm²)
0
50
100
150
200
0
100
200
300
400

FIG. 5B

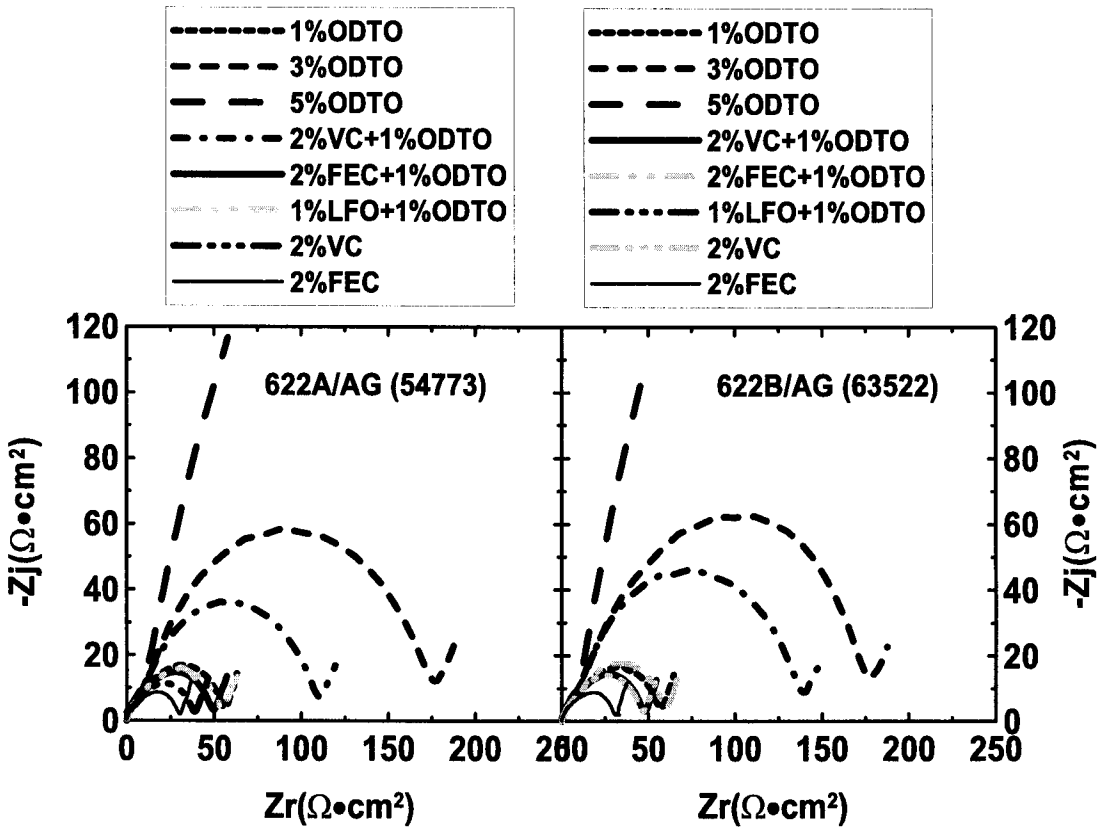
1%ODTO
3%ODTO
5%ODTO
2%VC+1%ODTO
2%FEC+1%ODTO
1%LFO+1%ODTO
2%VC
2%FEC
622A/AG (54773)
622B/AG (63522)
-Zj(Ω•cm²)
Zr(Ω•cm²)
0
20
40
60
80
100
120
0
50
100
150
200
250

FIG. 5C FIG. 5D

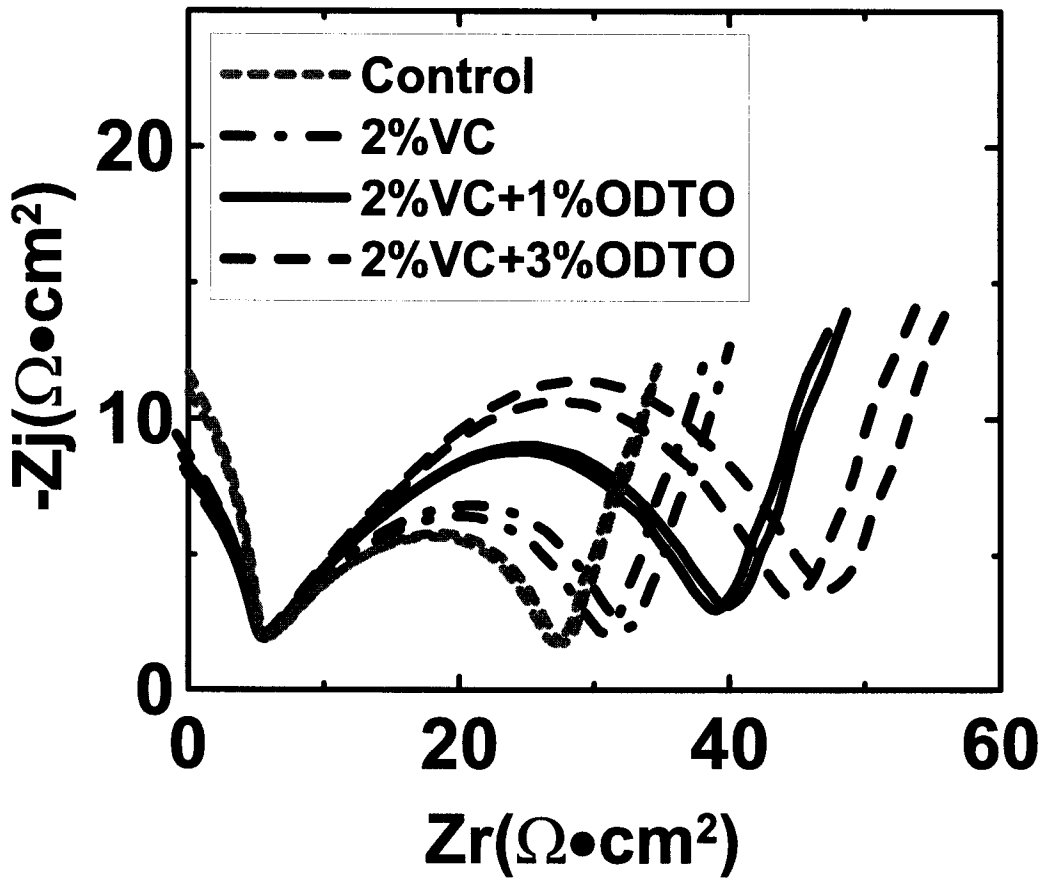
Control
2%VC
2%VC+1%ODTO
2%VC+3%ODTO
-Zj(Ω•cm²)
Zr(Ω•cm²)
0
10
20
0
20
40
60

FIG. 5E

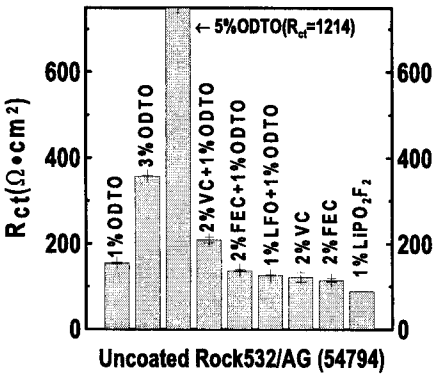

FIG. 6A

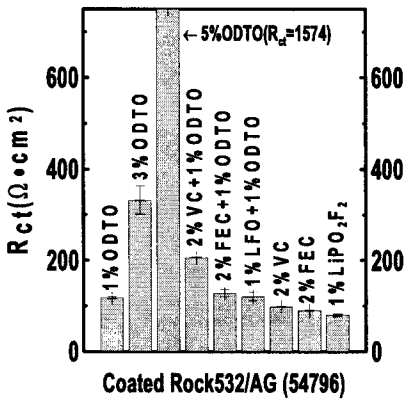

FIG. 6B

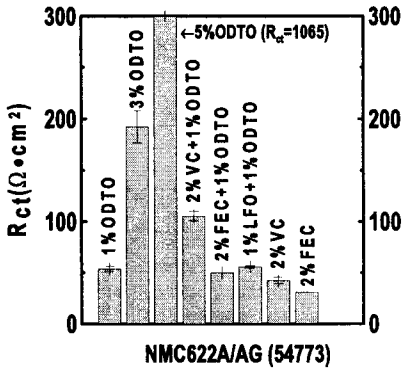

FIG. 6C

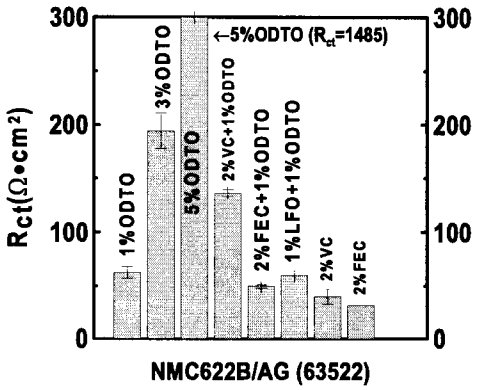

FIG. 6D

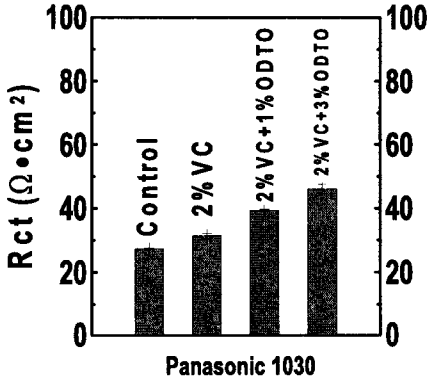

FIG. 6E

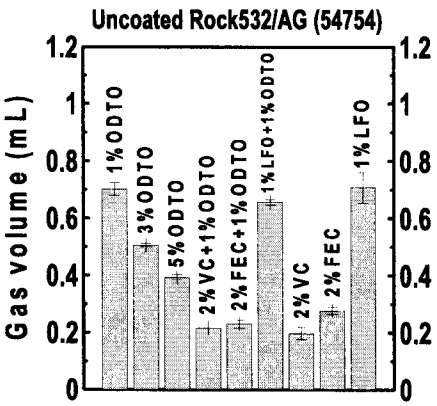

FIG. 7A

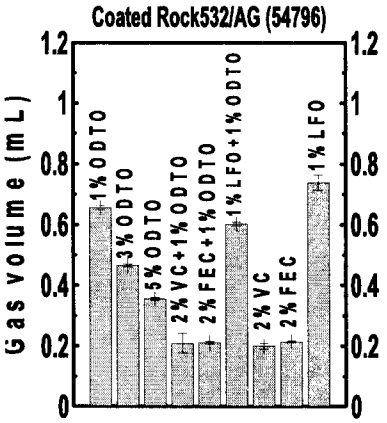

FIG. 7B

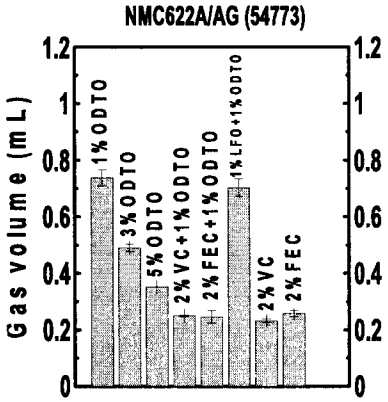

FIG. 7C

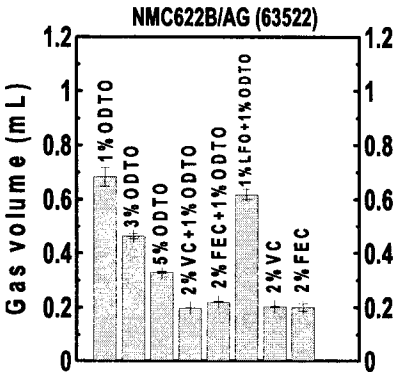

FIG. 7D

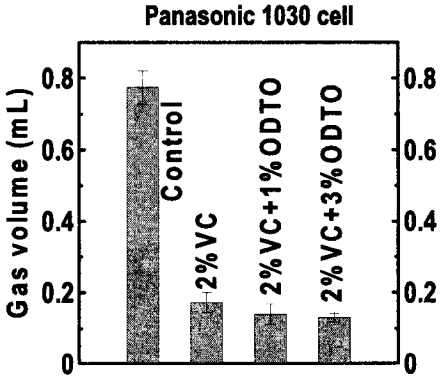

FIG. 7E

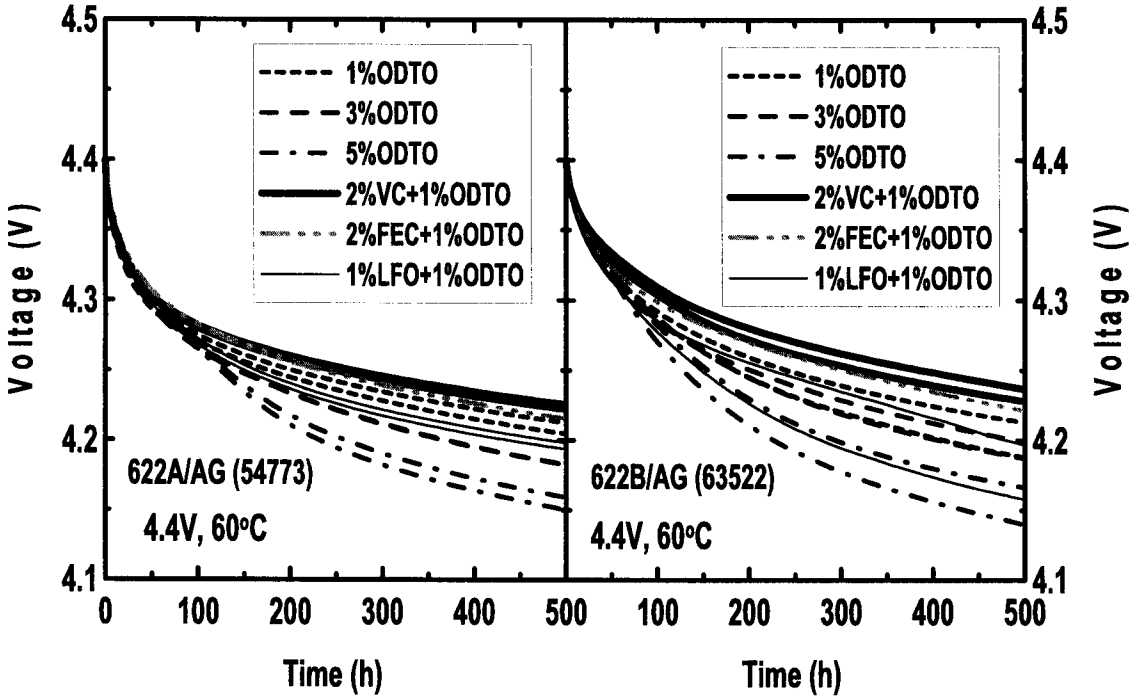
4.5
4.4
4.3
4.2
4.1
Voltage (V)
1%ODTO
3%ODTO
5%ODTO
2%VC+1%ODTO
2%FEC+1%ODTO
1%LFO+1%ODTO
622A/AG (54773)
4.4V, 60°C
0
100
200
300
400
500
Time (h)
622B/AG (63522)
4.4V, 60°C

FIG. 8A FIG. 8B

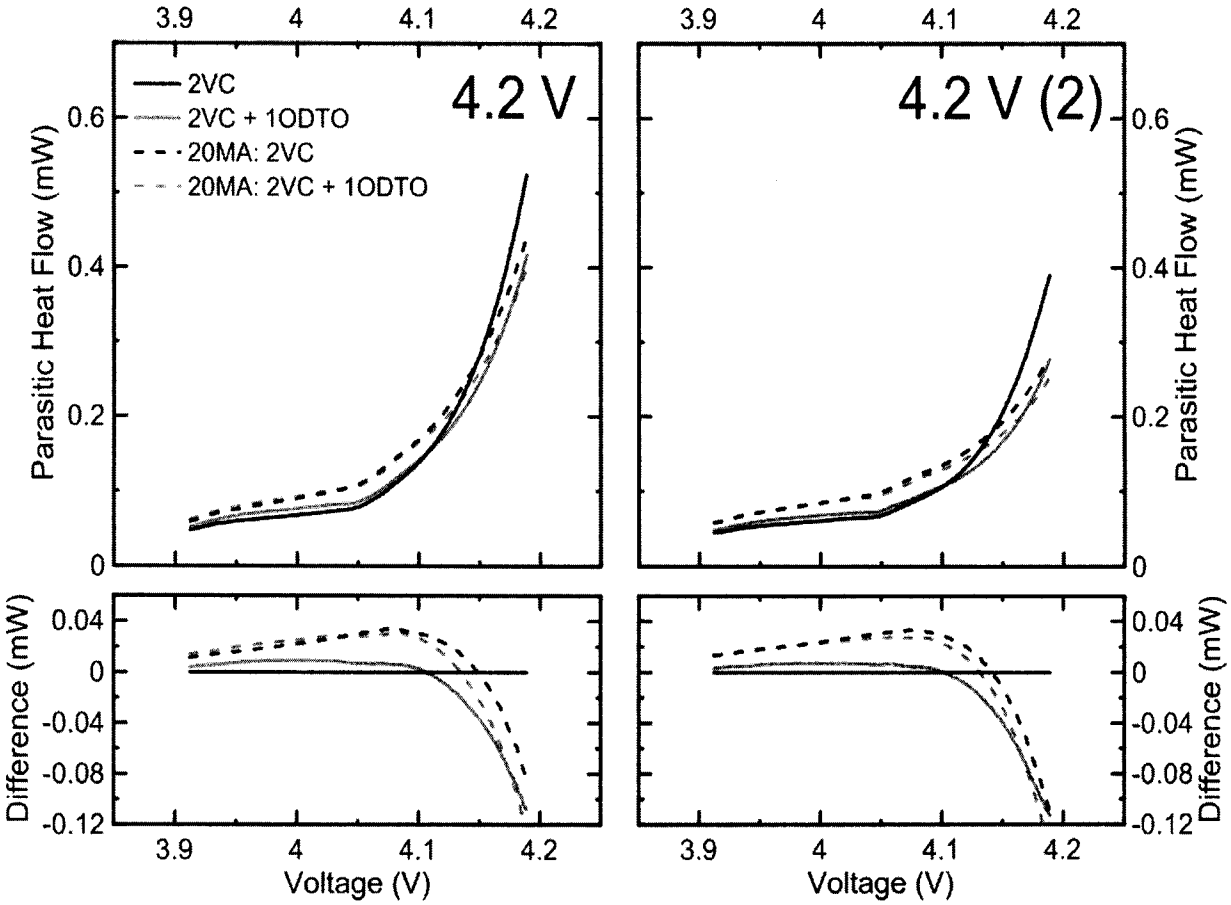
4.2 V
4.2 V (2)
2VC
2VC + 1ODTO
20MA: 2VC
20MA: 2VC + 1ODTO
Parasitic Heat Flow (mW)
Difference (mW)
Voltage (V)
3.9
4
4.1
4.2
0
0.2
0.4
0.6
0.04
-0.04
-0.08
-0.12

FIG. 9

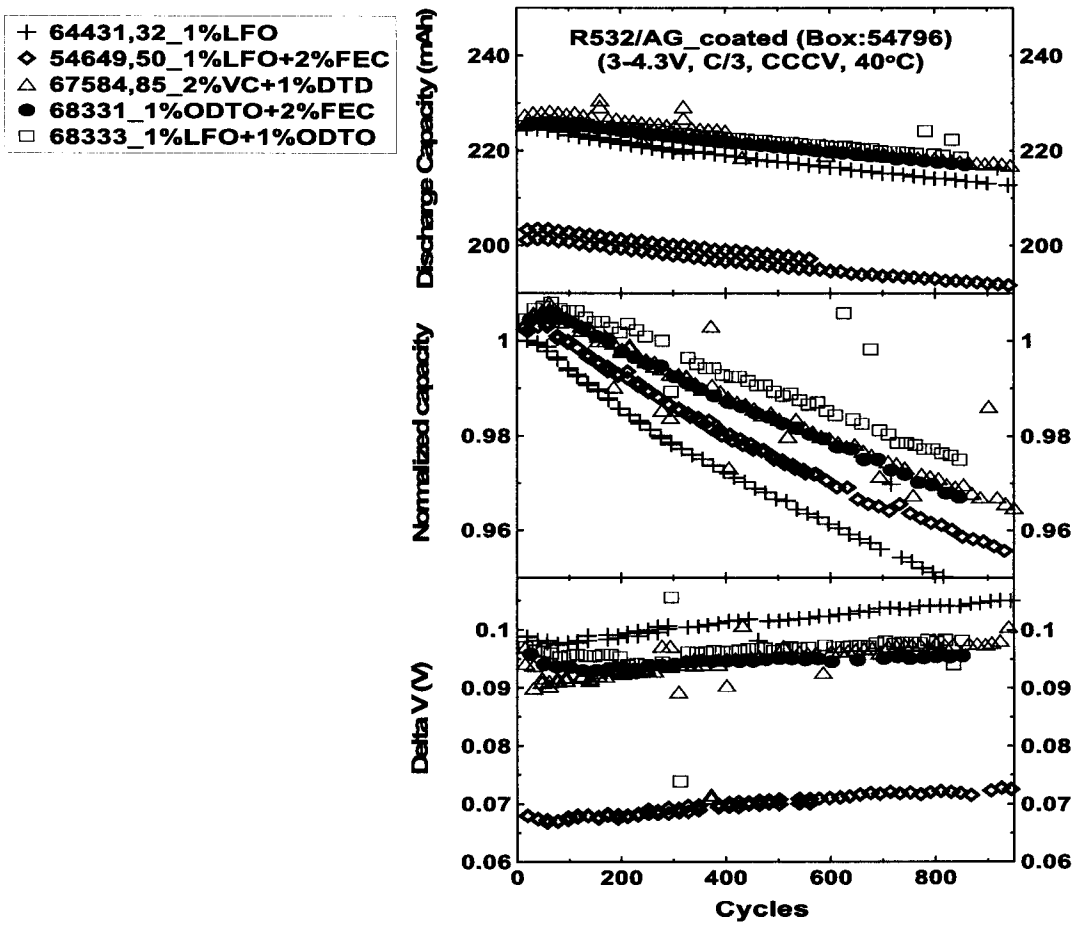
64431,32_1%LFO
54649,50_1%LFO+2%FEC
67584,85_2%VC+1%DTD
68331_1%ODTO+2%FEC
68333_1%LFO+1%ODTO
R532/AG_coated (Box:54796)
(3-4.3V, C/3, CCCV, 40°C)
Discharge Capacity (mAh)
Normalized capacity
Delta V (V)
Cycles
240
220
200
1
0.98
0.96
0.1
0.09
0.08
0.07
0.06
0
200
400
600
800

FIG. 10A

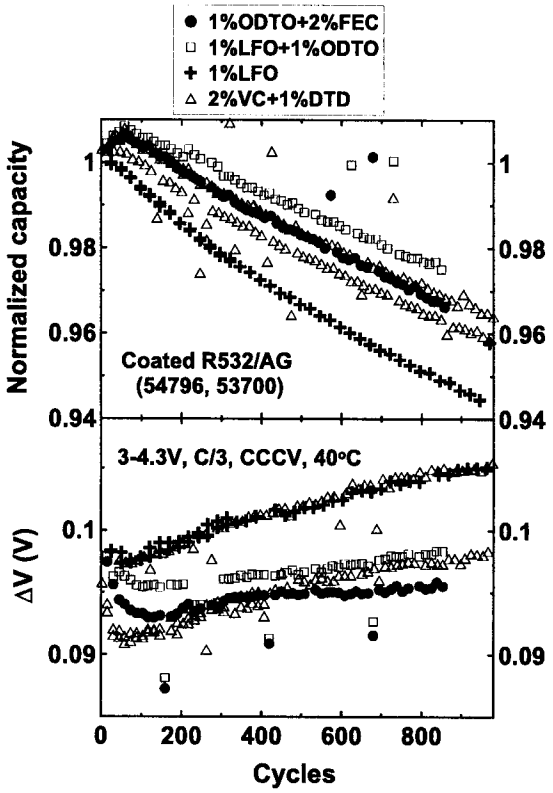

FIG. 10B

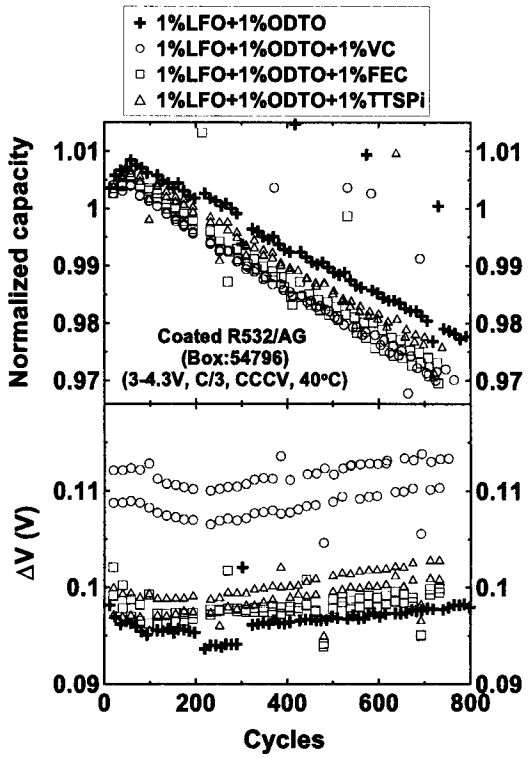

FIG. 10C

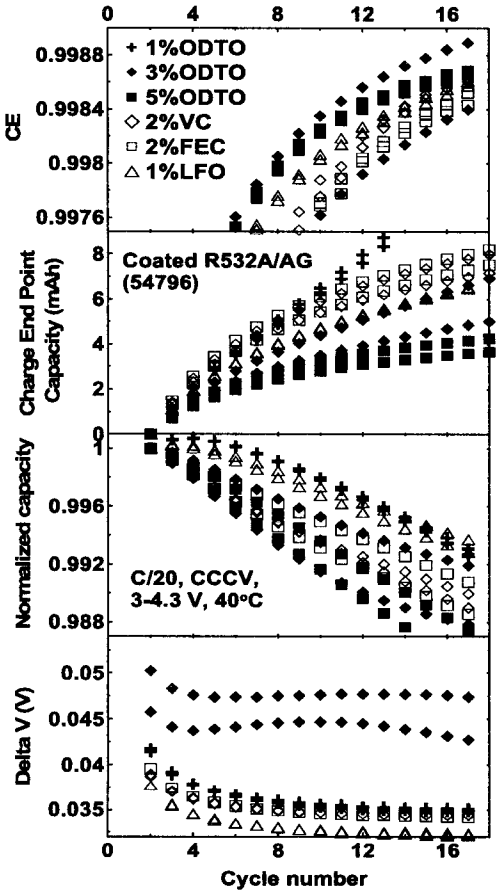

FIG. 10D

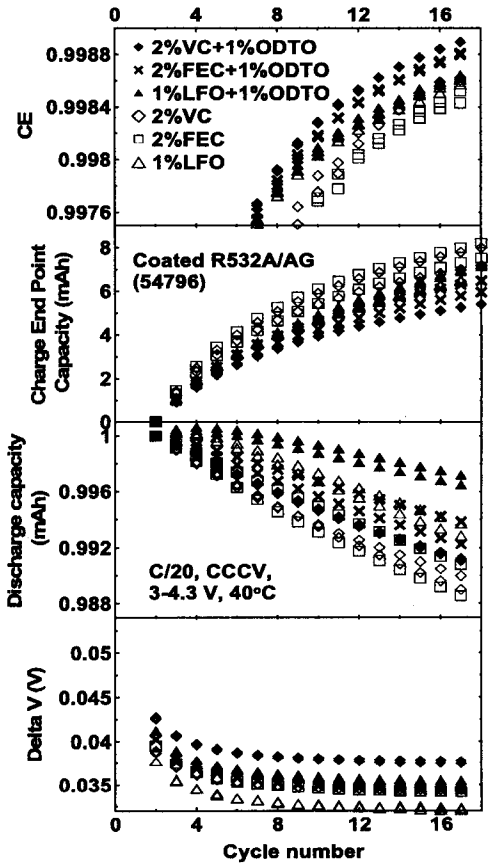

FIG. 10E

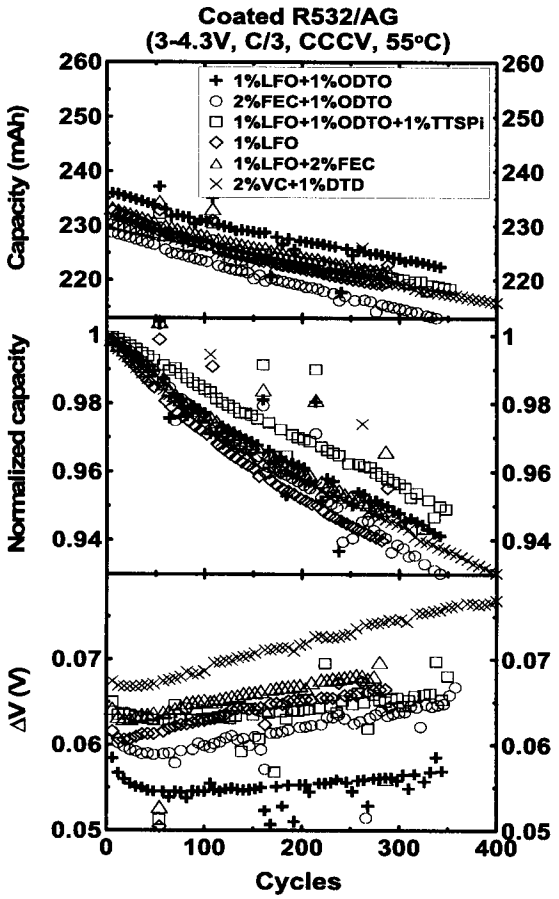

FIG. 10F

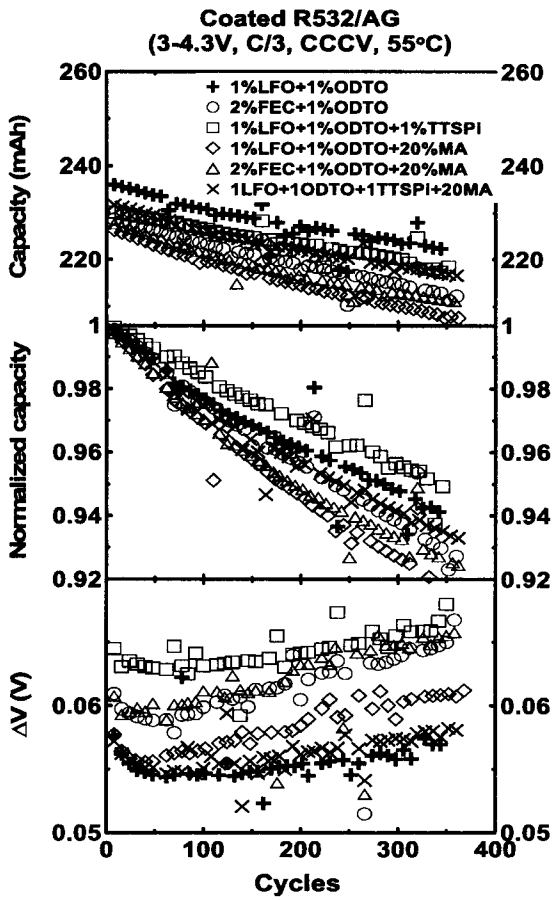

FIG. 10G

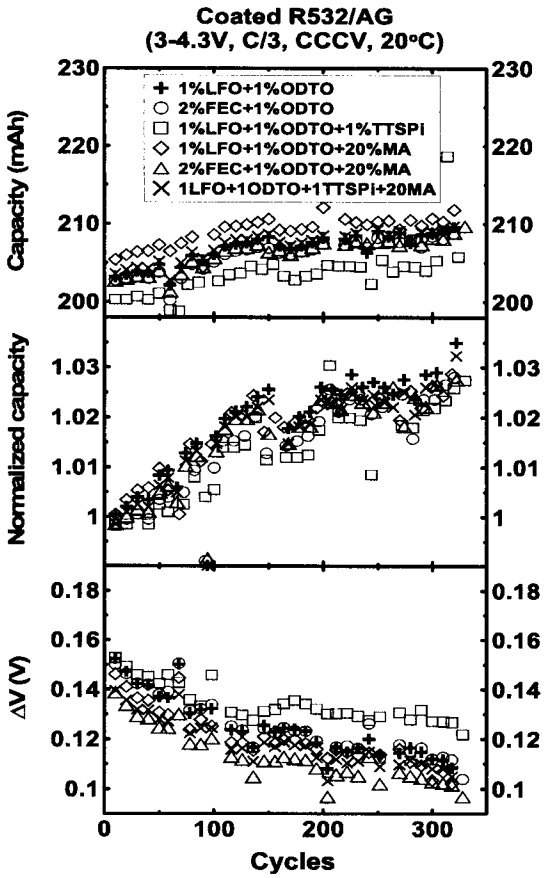

FIG. 10H

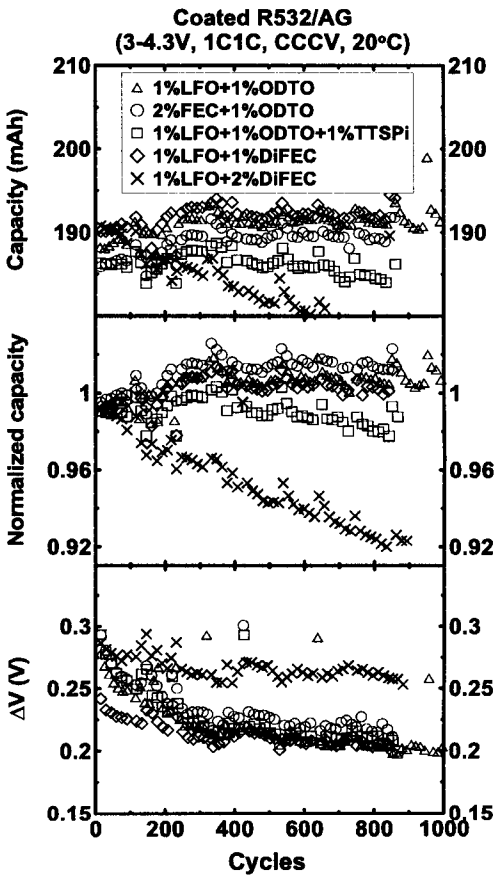

FIG. 10I

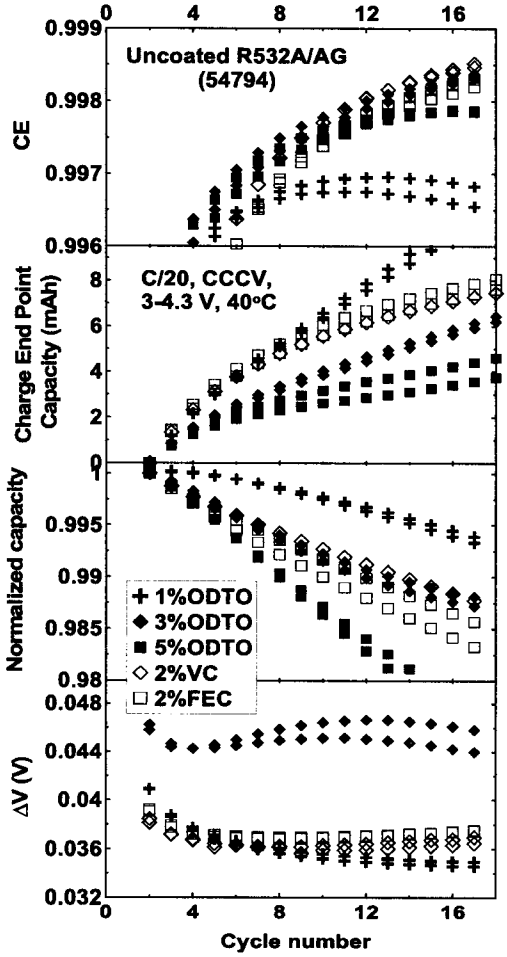

FIG. 10J

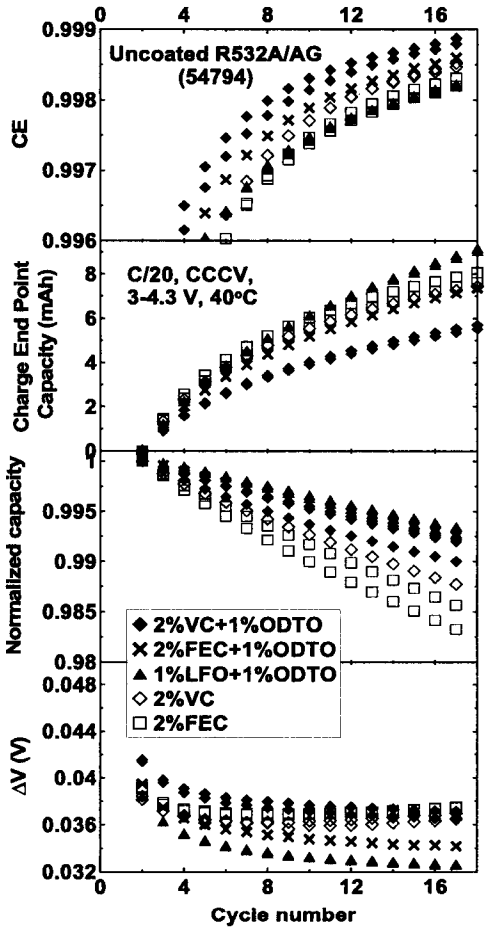

FIG. 10K

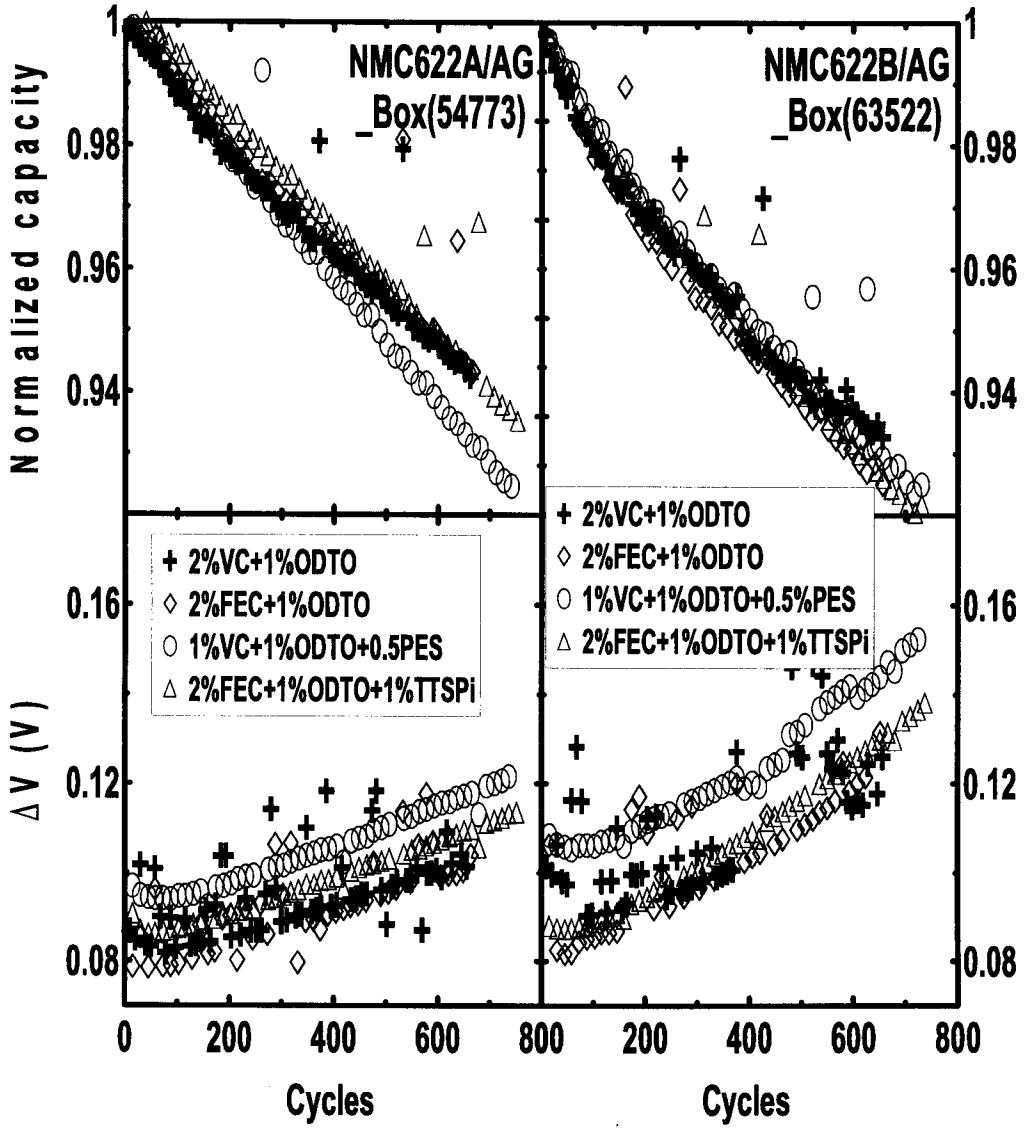

FIG. 10L

FIG. 10M

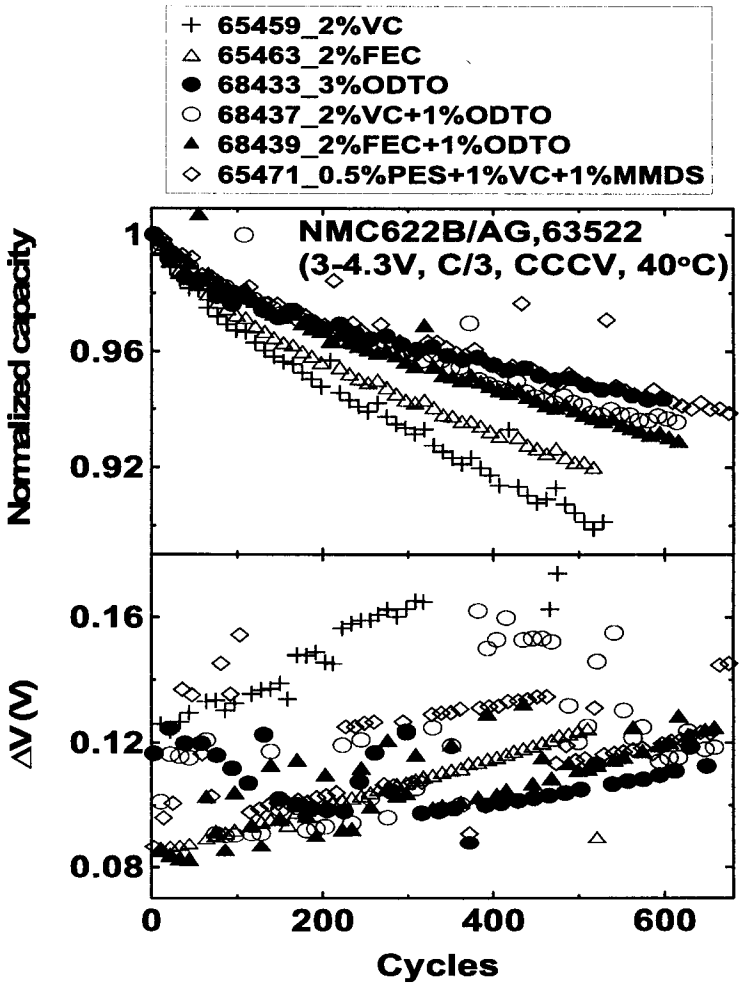
65459_2%VC
65463_2%FEC
68433_3%ODTO
68437_2%VC+1%ODTO
68439_2%FEC+1%ODTO
65471_0.5%PES+1%VC+1%MMDS
NMC622B/AG,63522
(3-4.3V, C/3, CCCV, 40°C)
Normalized capacity
0.96
0.92
ΔV (V)
0.16
0.12
0.08
0
200
400
600
Cycles

FIG. 10N

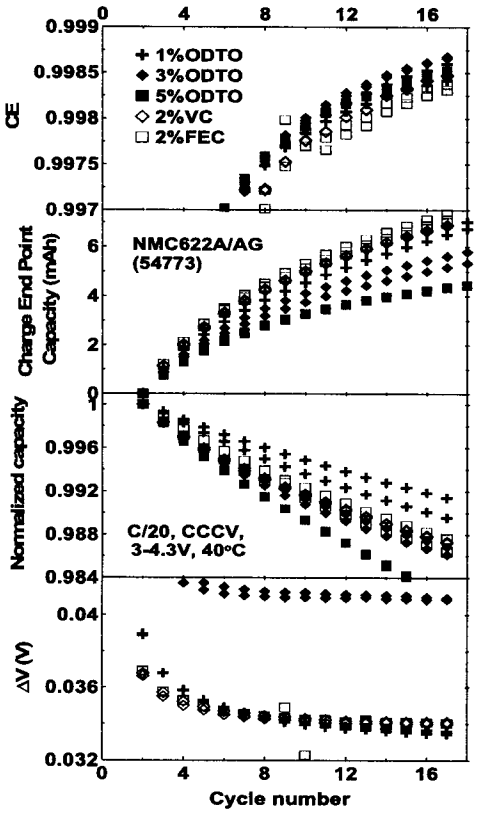

FIG. 10O

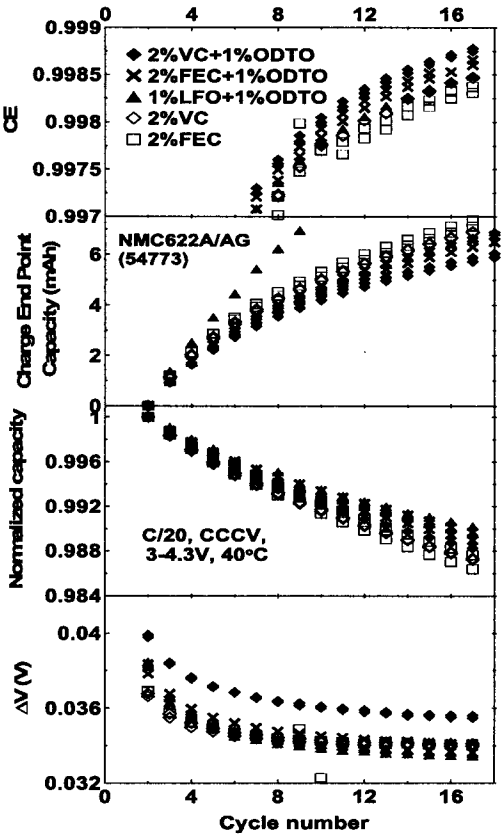

FIG. 10P

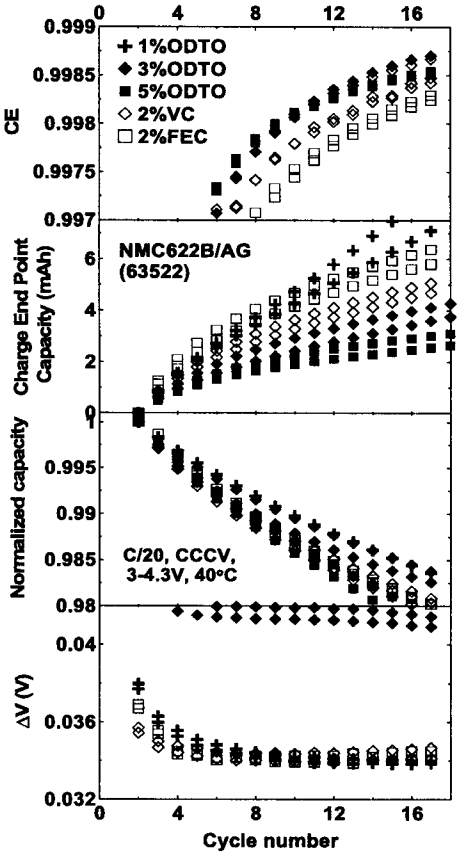

FIG. 10Q

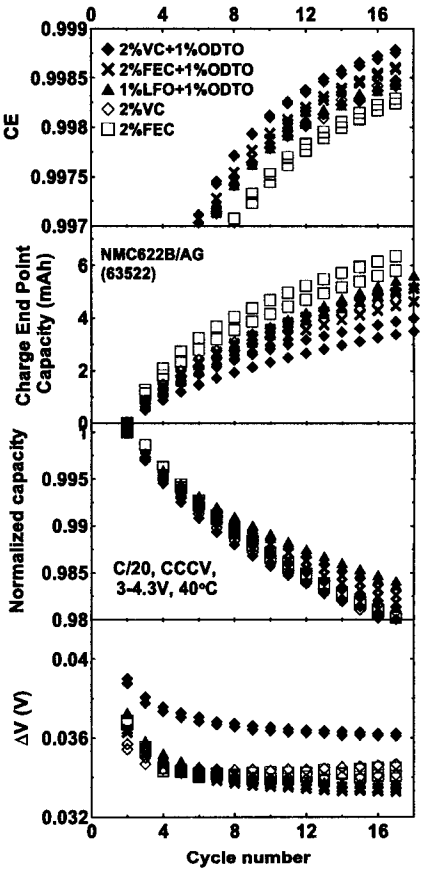

FIG. 10R

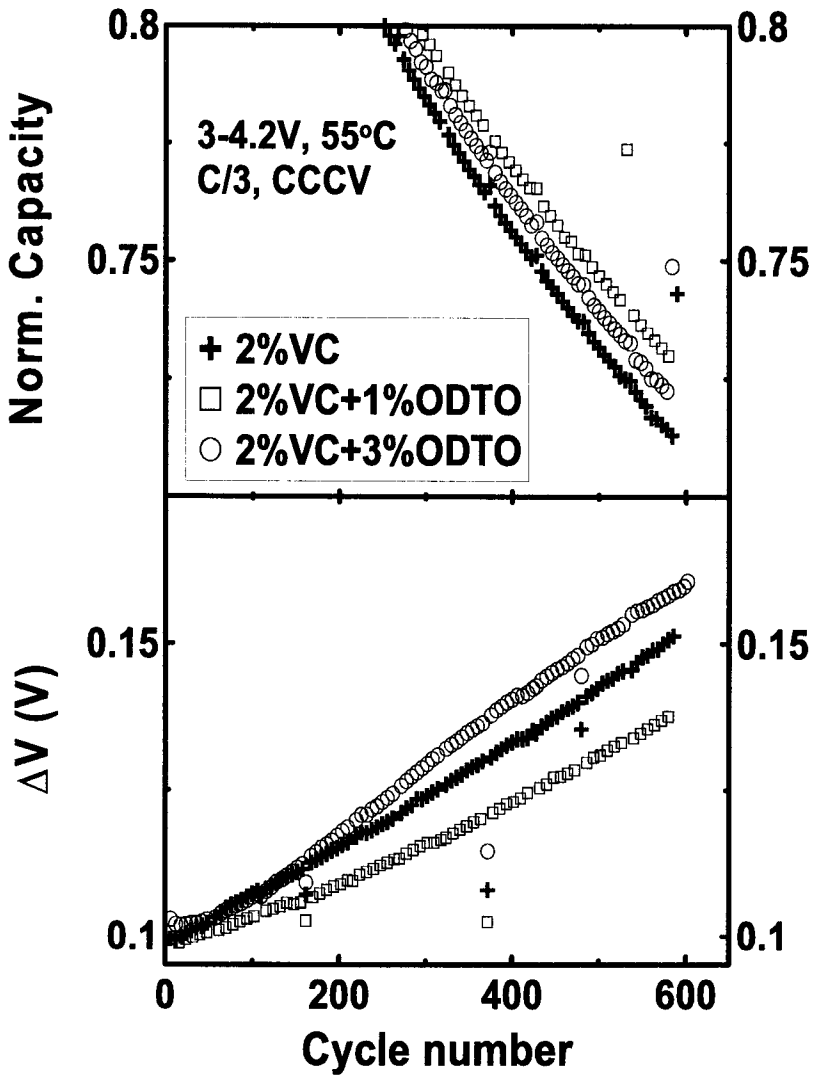
0.8
0.75
Norm. Capacity
3-4.2V, 55°C
C/3, CCCV
+ 2%VC
□ 2%VC+1%ODTO
○ 2%VC+3%ODTO
0.15
0.1
ΔV (V)
0
200
400
600
Cycle number

FIG. 10S

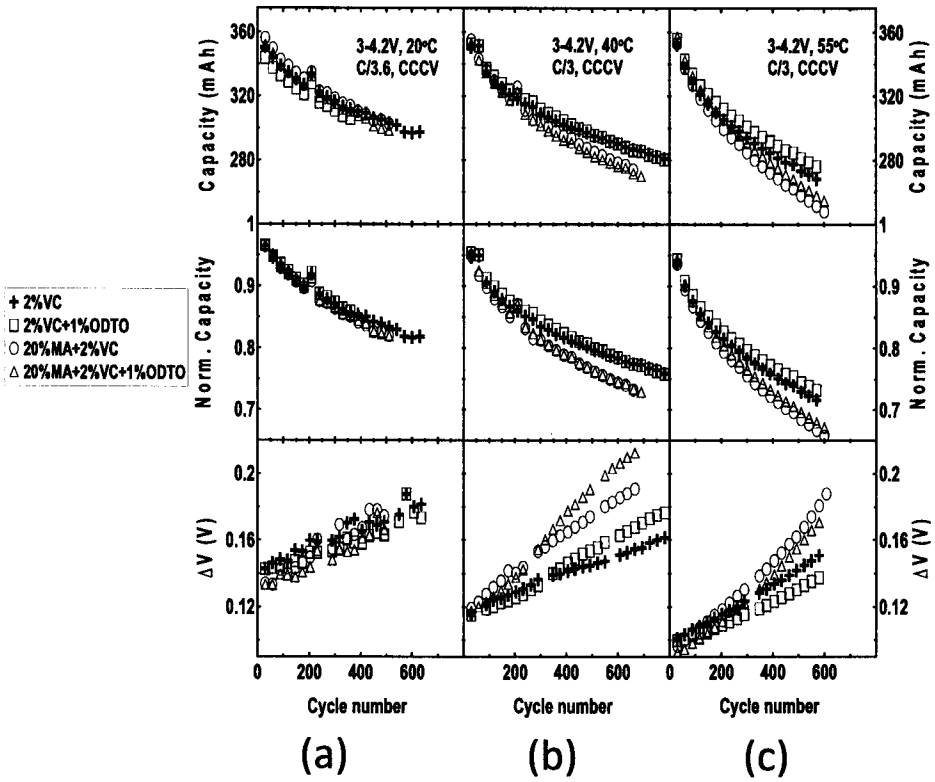
+ 2%VC
□ 2%VC+1%ODTO
○ 20%MA+2%VC
△ 20%MA+2%VC+1%ODTO
3-4.2V, 20°C
C/3.6, CCCV
3-4.2V, 40°C
C/3, CCCV
3-4.2V, 55°C
C/3, CCCV
Capacity (mAh)
Norm. Capacity
ΔV (V)
Cycle number
(a)
(b)
(c)

FIG. 10T

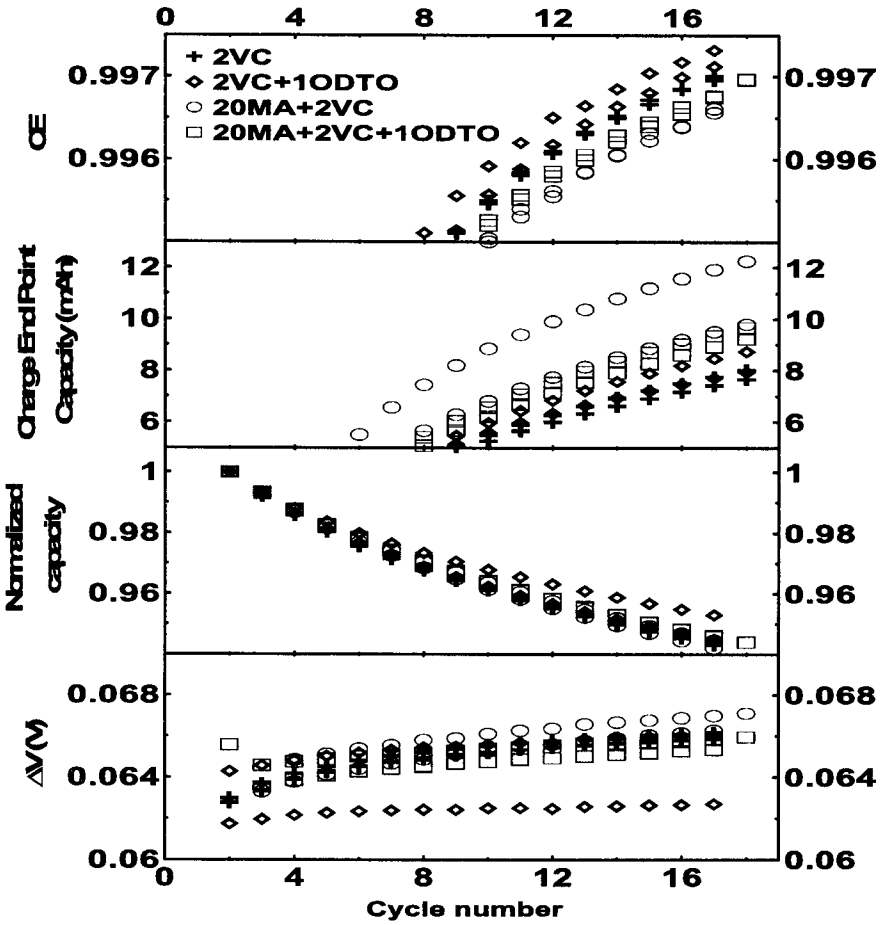
2VC
2VC+1ODTO
20MA+2VC
20MA+2VC+1ODTO
CE
Charge End Point Capacity (mAh)
Normalized capacity
ΔV(V)
Cycle number

FIG. 10U

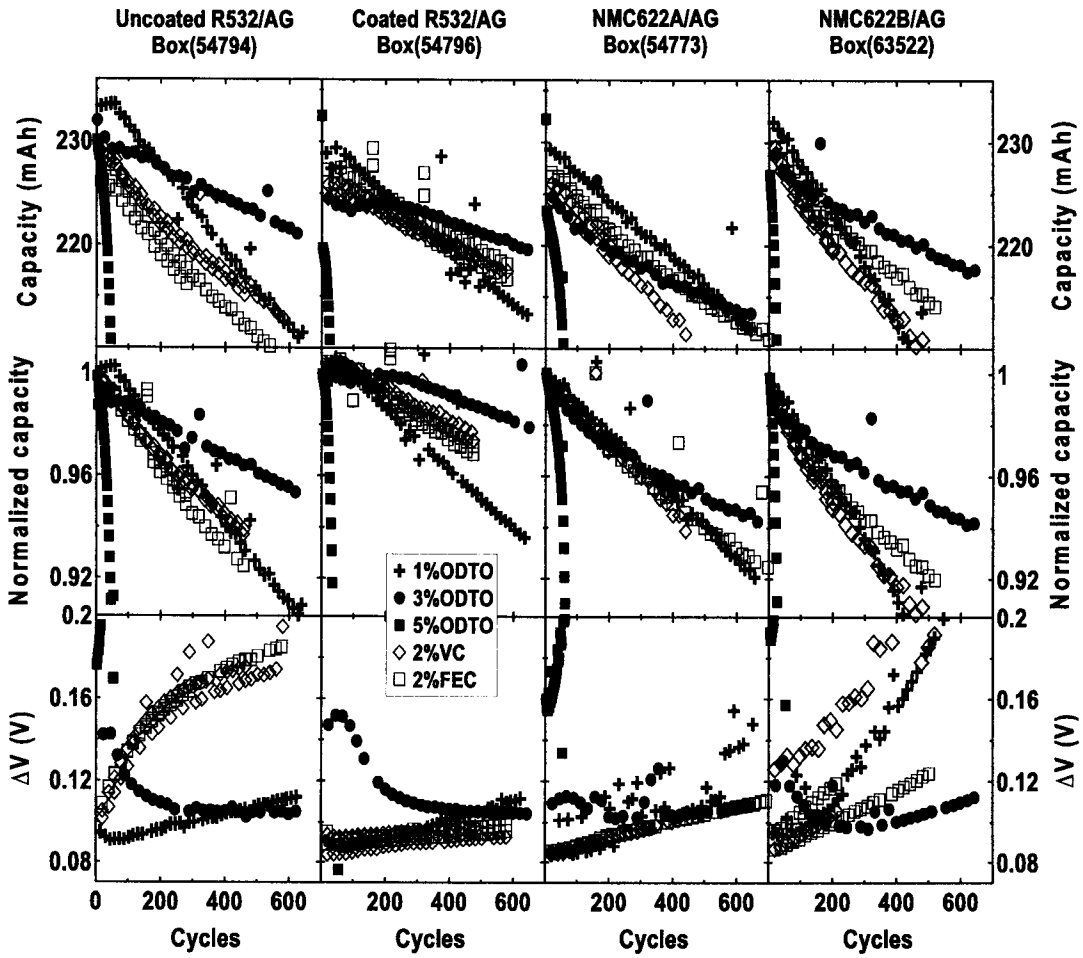
Uncoated R532/AG Box(54794)
Coated R532/AG Box(54796)
NMC622A/AG Box(54773)
NMC622B/AG Box(63522)
Capacity (mAh)
Normalized capacity
ΔV (V)
1%ODTO
3%ODTO
5%ODTO
2%VC
2%FEC
Cycles
(a)
(b)
(c)
(d)

FIG. 10V

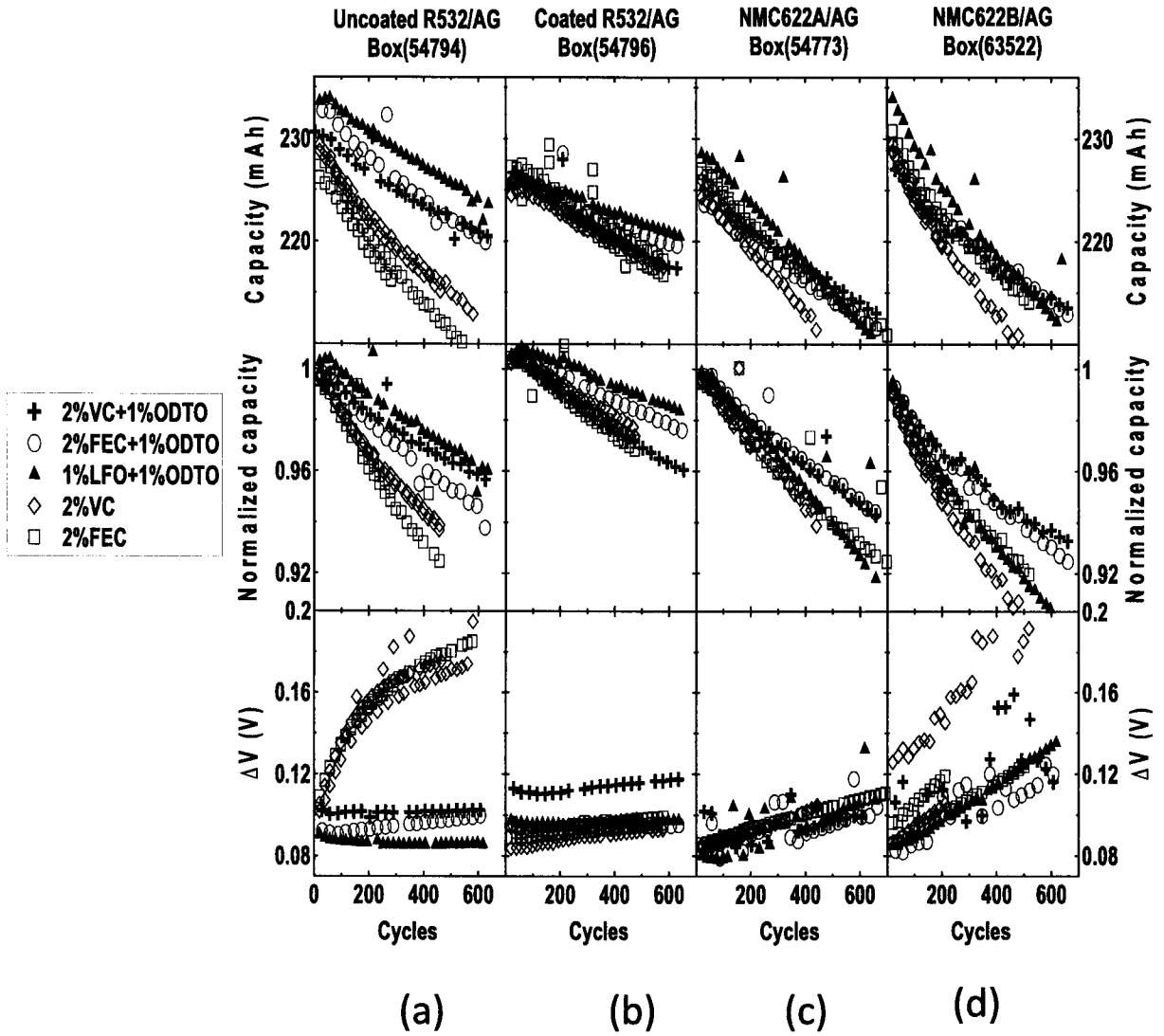
Uncoated R532/AG Box(54794)
Coated R532/AG Box(54796)
NMC622A/AG Box(54773)
NMC622B/AG Box(63522)
2%VC+1%ODTO
2%FEC+1%ODTO
1%LFO+1%ODTO
2%VC
2%FEC
Capacity (mAh)
Normalized capacity
ΔV (V)
Cycles
(a)
(b)
(c)
(d)

FIG. 10W

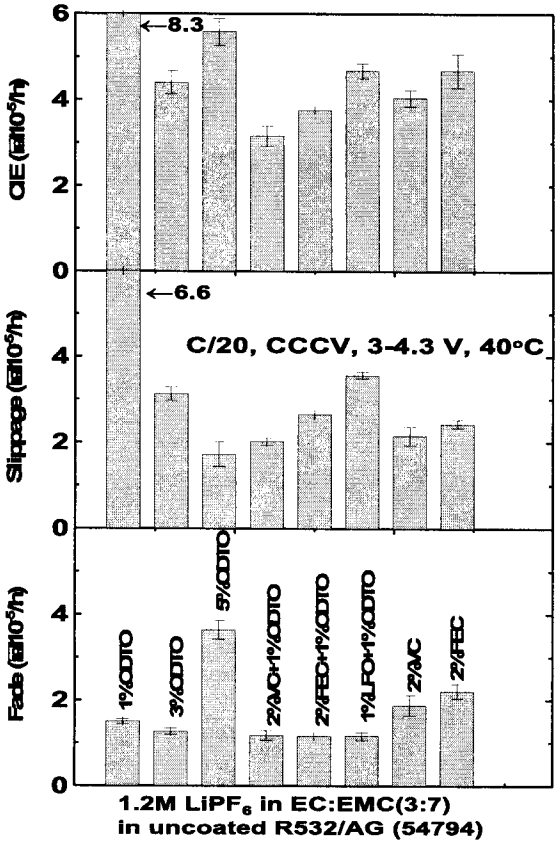
CE (%10⁻⁵/h)
Slippage (%10⁻⁵/h)
Fade (%10⁻⁵/h)
←8.3
←6.6
C/20, CCCV, 3-4.3 V, 40°C
1%ODTO
3%ODTO
5%ODTO
2%VC+1%ODTO
2%FEC+1%ODTO
1%LFO+1%ODTO
2%VC
2%FEC
1.2M LiPF6 in EC:EMC(3:7)
in uncoated R532/AG (54794)

FIG. 11

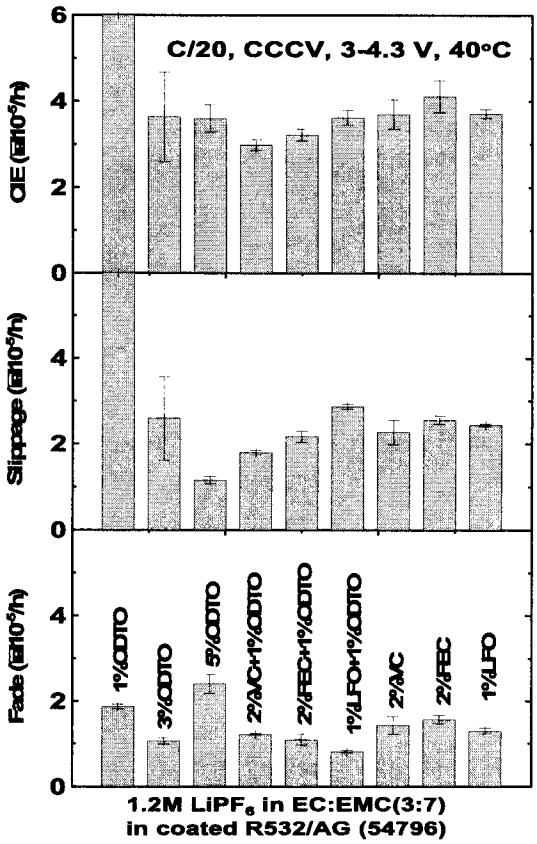
CE (%10⁻⁵/h)
Slippage (%10⁻⁵/h)
Fade (%10⁻⁵/h)
C/20, CCCV, 3-4.3 V, 40°C
1%ODTO
3%ODTO
5%ODTO
2%VC+1%ODTO
2%FEC+1%ODTO
1%LFO+1%ODTO
2%VC
2%FEC
1%LFO
1.2M LiPF6 in EC:EMC(3:7)
in coated R532/AG (54796)

FIG. 12

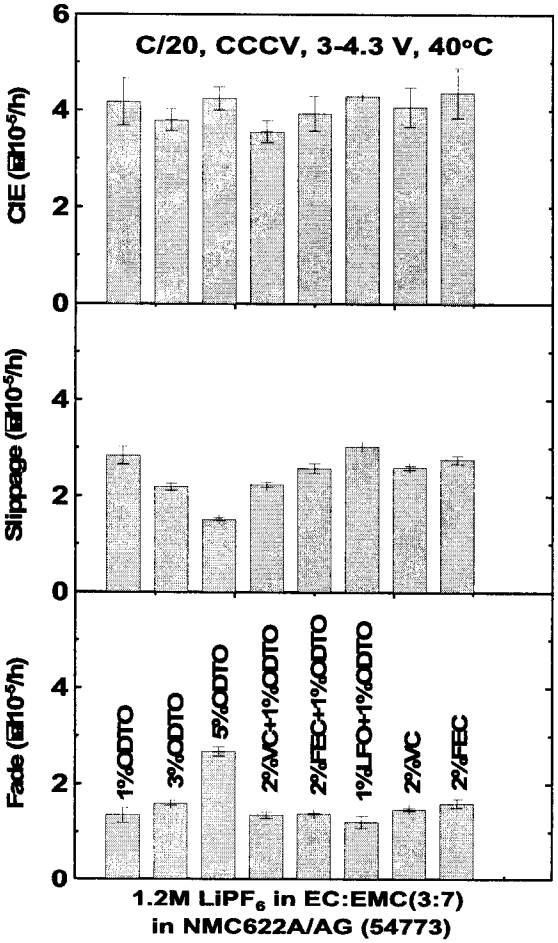
C/20, CCCV, 3-4.3 V, 40°C
CIE (10⁻⁵/h)
Slippage (10⁻⁵/h)
Fade (10⁻⁵/h)
1%ODTO
3%ODTO
5%ODTO
2%VC+1%ODTO
2%FEC+1%ODTO
1%LFO+1%ODTO
2%VC
2%FEC
1.2M LiPF6 in EC:EMC(3:7)
in NMC622A/AG (54773)

FIG. 13

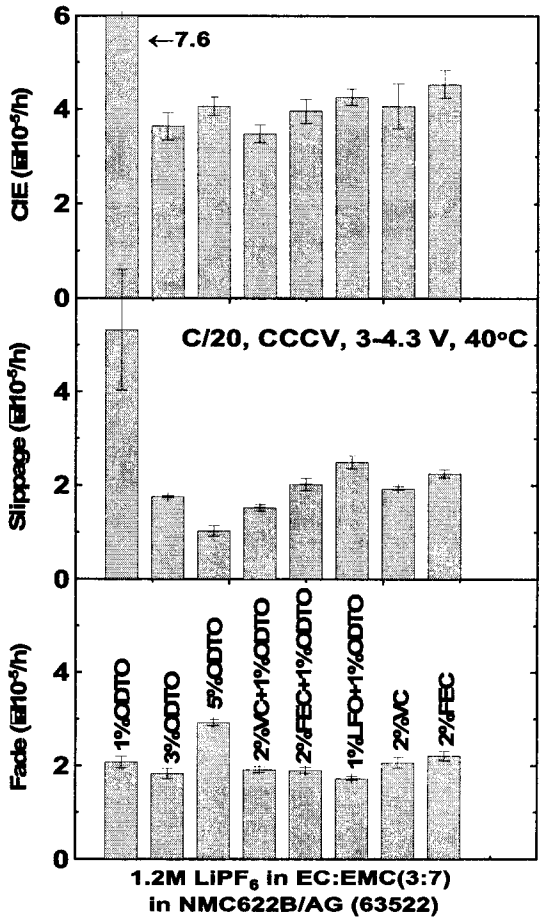
←7.6
C/20, CCCV, 3-4.3 V, 40°C
CIE (10⁻⁵/h)
Slippage (10⁻⁵/h)
Fade (10⁻⁵/h)
1%ODTO
3%ODTO
5%ODTO
2%VC+1%ODTO
2%FEC+1%ODTO
1%LFO+1%ODTO
2%VC
2%FEC
1.2M LiPF6 in EC:EMC(3:7)
in NMC622B/AG (63522)

FIG. 14

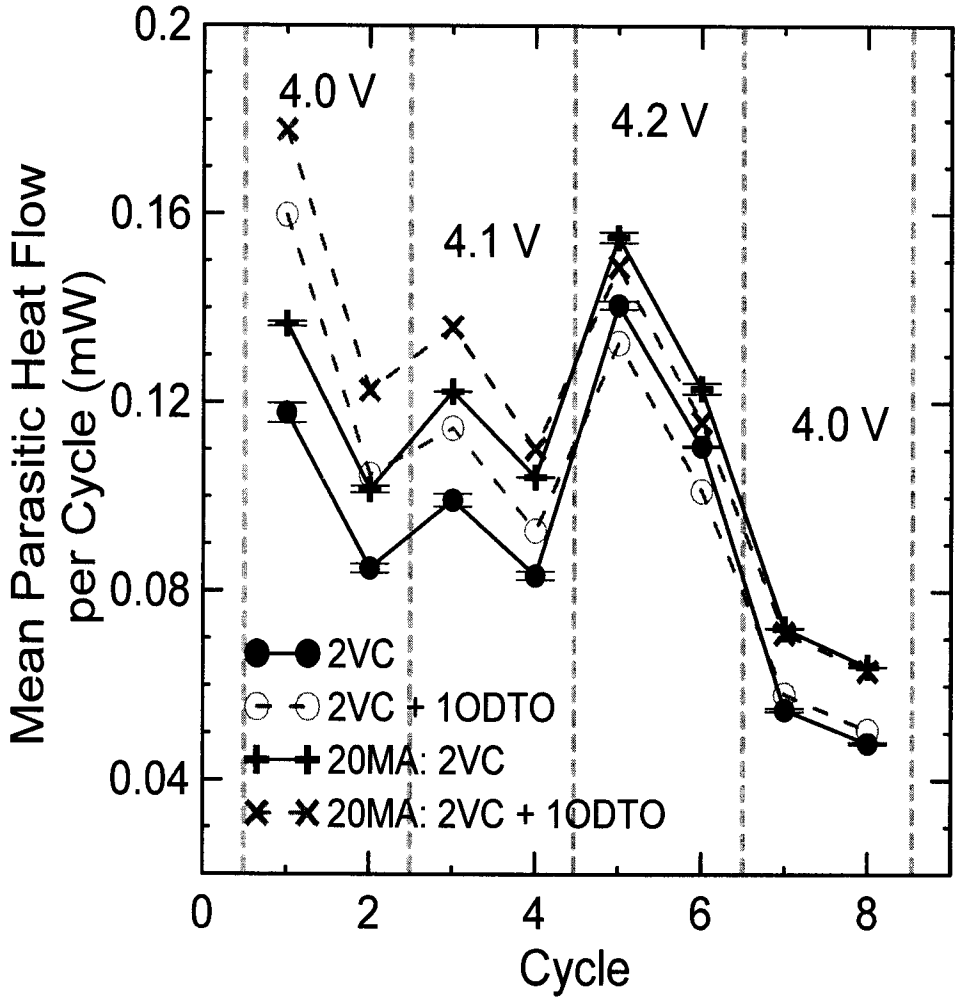
0.2
0.16
0.12
0.08
0.04
Mean Parasitic Heat Flow per Cycle (mW)
4.0 V
4.1 V
4.2 V
4.0 V
2VC
2VC + 1ODTO
20MA: 2VC
20MA: 2VC + 1ODTO
0
2
4
6
8
Cycle

FIG. 15

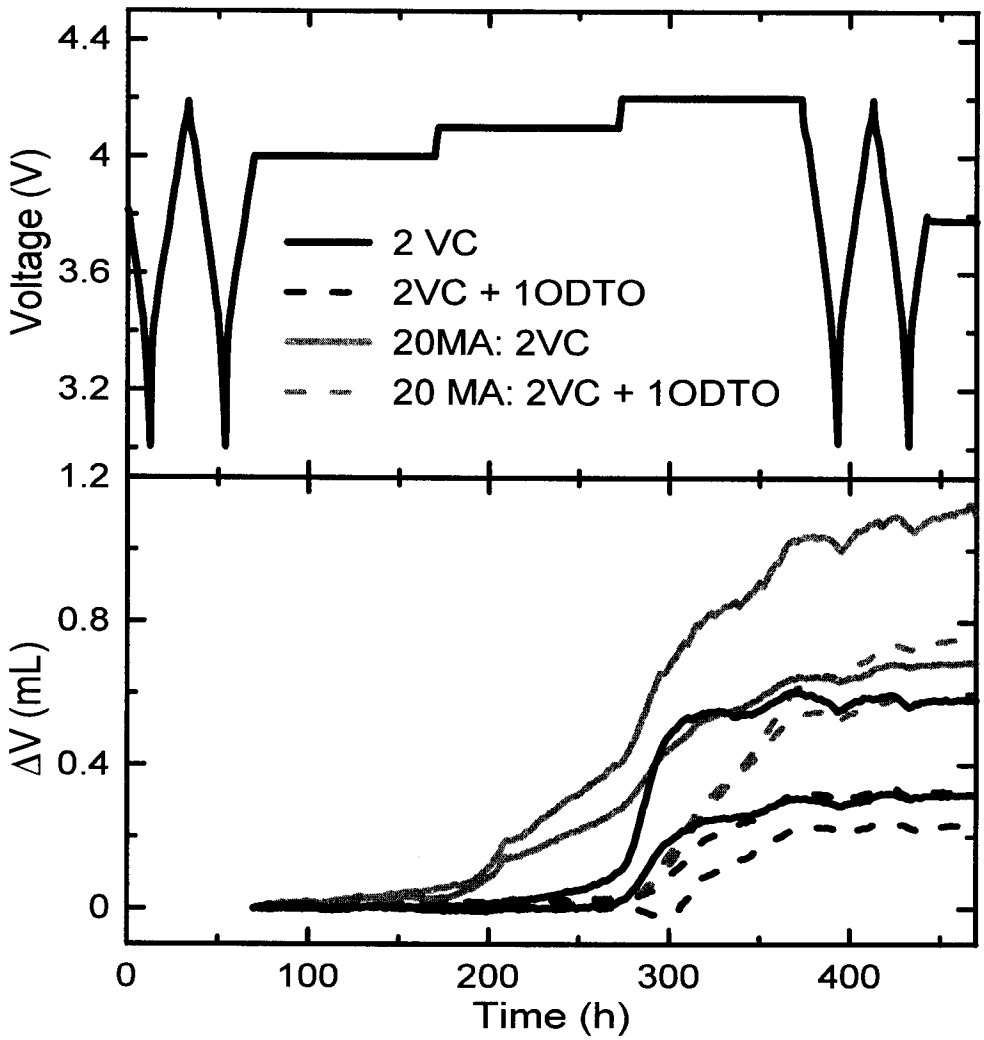
4.4
4
3.6
3.2
Voltage (V)
2 VC
2VC + 1ODTO
20MA: 2VC
20 MA: 2VC + 1ODTO
1.2
0.8
0.4
0
ΔV (mL)
0
100
200
300
400
Time (h)

FIG. 16

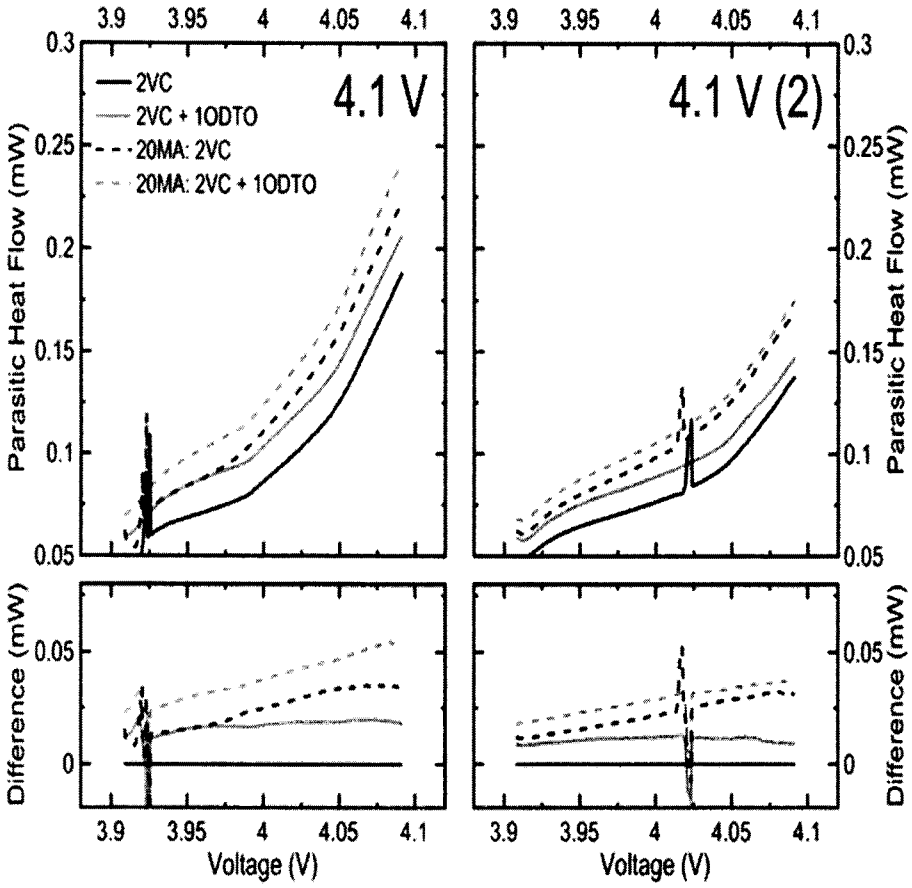
4.1 V
4.1 V (2)
2VC
2VC + 1ODTO
20MA: 2VC
20MA: 2VC + 1ODTO
Parasitic Heat Flow (mW)
Difference (mW)
Voltage (V)
3.9
3.95
4
4.05
4.1
0.3
0.25
0.2
0.15
0.1
0.05
0

FIG. 17

INTERNATIONAL SEARCH REPORT

International application No.
PCT/CA2018/000163

A. CLASSIFICATION OF SUBJECT MATTER
IPC: ***H01M 10/056*** (2010.01) , ***H01M 10/0525*** (2010.01)

According to International Patent Classification (IPC) or to both national classification and IPC

B. FIELDS SEARCHED

Minimum documentation searched (classification system followed by classification symbols)
IPC (2010.01): H01M 10/056, H01M 10/0525

Documentation searched other than minimum documentation to the extent that such documents are included in the fields searched
IPC (2006.01): H01M 10/40

Electronic database(s) consulted during the international search (name of database(s) and, where practicable, search terms used)
Databases: QUESTEL, Canadian Patent Database, SciFinder, CIPO Library Discovery Tool
Keywords: battery, cell, electrochemical, additive, solvent, solution, odto, oxodithiane+, oxodithiane+, dithiane+, disulfon+, disulphon+, propanedisulfon, or propanedisulphon+, carbonate, vc, vinylene, fec, fluoroethylene, fluoro ethylene, difluorophosphate, difluorodioxophosphate, phosphorodifluoridate, lipo2f2, lidfp, lfo, f2lio2p, lipf2o2

C. DOCUMENTS CONSIDERED TO BE RELEVANT

Category*	Citation of document, with indication, where appropriate, of the relevant passages	Relevant to claim No.
X	US 2017/0309891 Al (MATSUI et al.) 26 October 2017 (26-10-2017) *whole document*	1-36
X	US 2010/0178569 A1 (IHARA et al.) 15 July 2010 (15-07-2010) *whole document*	1-36
X A	US 8,940,439 B2 (KAWASHIMA et al.) 27 January 2015 (27-01-2015) *whole document*	1-6, 8-16, 18-29, 31-36 7, 17, 30
X A	US 2010/0216017 A1 (SAITO et al.) 26 August 2010 (26-08-2010) *whole document*	1-6, 8-16, 18-29, 31-36 7, 17, 30
X A	CN 105186032 (YANG et al.) 23 December 2015 (23-12-2015) *abstract and machine English translation of description*	1-6, 8-16, 18-29, 31-36 7, 17, 30

☑ Further documents are listed in the continuation of Box C. ☑ See patent family annex.

*	Special categories of cited documents:	"T"	later document published after the international filing date or priority date and not in conflict with the application but cited to understand the principle or theory underlying the invention
"A"	document defining the general state of the art which is not considered to be of particular relevance	"X"	document of particular relevance; the claimed invention cannot be considered novel or cannot be considered to involve an inventive step when the document is taken alone
"E"	earlier application or patent but published on or after the international filing date	"Y"	document of particular relevance; the claimed invention cannot be considered to involve an inventive step when the document is combined with one or more other such documents, such combination being obvious to a person skilled in the art
"L"	document which may throw doubts on priority claim(s) or which is cited to establish the publication date of another citation or other special reason (as specified)	"&"	document member of the same patent family
"O"	document referring to an oral disclosure, use, exhibition or other means		
"P"	document published prior to the international filing date but later than the priority date claimed		

Date of the actual completion of the international search 28 November 2018 (28-11-2018)	Date of mailing of the international search report 17 December 2018 (17-12-2018)
Name and mailing address of the ISA/CA Canadian Intellectual Property Office Place du Portage I, C114 - 1st Floor, Box PCT 50 Victoria Street Gatineau, Quebec K1A 0C9 Facsimile No.: 819-953-2476	Authorized officer Philip Gbor (819) 639-8475

C (Continuation). DOCUMENTS CONSIDERED TO BE RELEVANT

Category*	Citation of document, with indication, where appropriate, of the relevant passages	Relevant to claim No.
A	US 2010/0190065 A1 (IHARA et al.) 29 July 2010 (29-07-2010) *whole document*	1-36
A	WO 2017/026181 A1 (ITABASHI et al.) 16 February 2017 (16-02-2017) *whole document*	1-36
A	US 7,163,768 B2 (UTSUGI et al.) 16 January 2007 (16-01-2007) *whole document*	1-36
A	US 2012/0058401 A1 (IHARA et al.) 8 March 2012 (08-03-2012) *whole document*	1-36
A	US 2018/0034011 A1 (TSUDA et al.) 1 February 2018 (01-02-2018) *whole document*	1-36
A	US 9,912,013 (HAYAKAWA et al.) 6 March 2018 (06-03-2018) *whole document*	1-36
A	US 9,455,476 B2 (IHARA et al.) 27 September 2016 (27-09-2016) *whole document*	1-36

INTERNATIONAL SEARCH REPORT

International application No.
PCT/CA2018/000163

Box No. II Observations where certain claims were found unsearchable (Continuation of item 2 of the first sheet)

This international search report has not been established in respect of certain claims under Article 17(2)(a) for the following reasons:

1. ☐ Claim Nos.:
because they relate to subject matter not required to be searched by this Authority, namely:

2. ☐ Claim Nos.:
because they relate to parts of the international application that do not comply with the prescribed requirements to such an extent that no meaningful international search can be carried out, specifically:

3. ☐ Claim Nos.:
because they are dependent claims and are not drafted in accordance with the second and third sentences of Rule 6.4(a).

Box No. III Observations where unity of invention is lacking (Continuation of item 3 of first sheet)

This International Searching Authority found multiple inventions in this international application, as follows:
See extra sheet

1. ☑ As all required additional search fees were timely paid by the applicant, this international search report covers all searchable claims.

2. ☐ As all searchable claims could be searched without effort justifying additional fees, this Authority did not invite payment of additional fees.

3. ☐ As only some of the required additional search fees were timely paid by the applicant, this international search report covers only those claims for which fees were paid, specifically claim Nos.:

4. ☐ No required additional search fees were timely paid by the applicant. Consequently, this international search report is restricted to the invention first mentioned in the claims; it is covered by claim Nos.:

Remark on Protest

☐ The additional search fees were accompanied by the applicant's protest and, where applicable, the payment of a protest fee.

☐ The additional search fees were accompanied by the applicant's protest but the applicable protest fee was not paid within the time limit specified in the invitation.

☑ No protest accompanied the payment of additional search fees.

Continuation of: Box No. III

The International Searching Authority found multiple (groups of) inventions in this international application, as follows:

Group A - Claims 1-4(part), 5-6, 8-14(part), 15-16, 18-27(part), 28-29 and 31-36(part) are directed to a nonaqueous electrolyte and a lithium-ion battery which contains the nonaqueous electrolyte, the nonaqueous electrolyte comprising lithium salt, a nonaqueous solvent, and an additive mixture comprising a first operative additive that is vinylene carbonate or fluoroethylene carbonate, or any combination of them, and a second operative additive that is l,2,6-oxodithiane-2,2,6,6-tetraoxide having the formula (I); and

Group B - Claims 1-4(part), 7, 8-14(part), 17, 18-27(part), 30 and 31-36(part) are directed to a nonaqueous electrolyte and a lithium-ion battery which contains the nonaqueous electrolyte, the nonaqueous electrolyte comprising lithium salt, a nonaqueous solvent, and an additive mixture comprising a first operative additive that is $LiPO_2F_2$ and a second operative additive that is l,2,6-oxodithiane-2,2,6,6-tetraoxide having the formula (I).

INTERNATIONAL SEARCH REPORT
Information on patent family members

International application No.
PCT/CA2018/000163

Patent Document Cited in Search Report	Publication Date	Patent Family Member(s)	Publication Date
US2017309891A1	26 October 2017 (26-10-2017)	US2017309891A1	26 October 2017 (26-10-2017)
		CN107004854A	01 August 2017 (01-08-2017)
		JP2016105366A	09 June 2016 (09-06-2016)
		WO2016088471A1	09 June 2016 (09-06-2016)
US2010178569A1	15 July 2010 (15-07-2010)	US2010178569A1	15 July 2010 (15-07-2010)
		US9012095B2	21 April 2015 (21-04-2015)
		CN101783412A	21 July 2010 (21-07-2010)
		CN101783412B	02 January 2013 (02-01-2013)
		EP2211401A2	28 July 2010 (28-07-2010)
		EP2211401A3	27 October 2010 (27-10-2010)
		EP2211401B1	20 March 2013 (20-03-2013)
		JP2010165542A	29 July 2010 (29-07-2010)
US8940439B2	27 January 2015 (27-01-2015)	US2012244410A1	27 September 2012 (27-09-2012)
		US8940439B2	27 January 2015 (27-01-2015)
		CN102694161A	26 September 2012 (26-09-2012)
		CN102694161B	03 May 2017 (03-05-2017)
		EP2503632A1	26 September 2012 (26-09-2012)
		IN762DE2012A	21 August 2015 (21-08-2015)
		JP2012199172A	18 October 2012 (18-10-2012)
		JP5668929B2	12 February 2015 (12-02-2015)
		KR20120109316A	08 October 2012 (08-10-2012)
US2010216017A1	26 August 2010 (26-08-2010)	US2010216017A1	26 August 2010 (26-08-2010)
		US9509015B2	29 November 2016 (29-11-2016)
		CN101345326A	14 January 2009 (14-01-2009)
		CN101345326B	17 November 2010 (17-11-2010)
		JP2009038018A	19 February 2009 (19-02-2009)
		KR20090005973A	14 January 2009 (14-01-2009)
		US2009017374A1	15 January 2009 (15-01-2009)
		US8197964B2	12 June 2012 (12-06-2012)
CN105186032A	23 December 2015 (23-12-2015)	None	
US2010190065A1	29 July 2010 (29-07-2010)	US2010190065A1	29 July 2010 (29-07-2010)
		US8980483B2	17 March 2015 (17-03-2015)
		CN101789520A	28 July 2010 (28-07-2010)
		CN101789520B	27 February 2013 (27-02-2013)
		EP2211402A2	28 July 2010 (28-07-2010)
		EP2211402A3	27 October 2010 (27-10-2010)
		EP2211402B1	03 July 2013 (03-07-2013)
		JP2010170886A	05 August 2010 (05-08-2010)
WO2017026181A1	16 February 2017 (16-02-2017)	WO2017026181A1	16 February 2017 (16-02-2017)
		CN107851847A	27 March 2018 (27-03-2018)
		EP3333962A1	13 June 2018 (13-06-2018)
		EP3333962A4	13 June 2018 (13-06-2018)
		JP2017037808A	16 February 2017 (16-02-2017)
		JP6098684B2	22 March 2017 (22-03-2017)
		KR20180038038A	13 April 2018 (13-04-2018)

US7163768B2	16 January 2007 (16-01-2007)	US2004043300A1	04 March 2004 (04-03-2004)
		US7163768B2	16 January 2007 (16-01-2007)
		CN1495959A	12 May 2004 (12-05-2004)
		CN1280942C	18 October 2006 (18-10-2006)
		DE60304522D1	24 May 2006 (24-05-2006)
		DE60304522T2	14 December 2006 (14-12-2006)
		EP1394888A1	03 March 2004 (03-03-2004)
		EP1394888B1	12 April 2006 (12-04-2006)
		JP2004281368A	07 October 2004 (07-10-2004)
		JP4033074B2	16 January 2008 (16-01-2008)
		KR20040019994A	06 March 2004 (06-03-2004)
		KR100538901B1	27 December 2005 (27-12-2005)
US2012058401A1	08 March 2012 (08-03-2012)	US2012058401A1	08 March 2012 (08-03-2012)
		CN102386443A	21 March 2012 (21-03-2012)
		JP2012054156A	15 March 2012 (15-03-2012)
US2018034011A1	01 February 2018 (01-02-2018)	US2018034011A1	01 February 2018 (01-02-2018)
		JP2016154079A	25 August 2016 (25-08-2016)
		WO2016132675A1	25 August 2016 (25-08-2016)
US9912013B2	06 March 2018 (06-03-2018)	US2017098860A1	06 April 2017 (06-04-2017)
		US9912013B2	06 March 2018 (06-03-2018)
		CN102356499A	15 February 2012 (15-02-2012)
		CN102356499B	08 April 2015 (08-04-2015)
		CN104332655A	04 February 2015 (04-02-2015)
		CN104332655B	24 October 2017 (24-10-2017)
		EP2413417A1	01 February 2012 (01-02-2012)
		JP2010225522A	07 October 2010 (07-10-2010)
		US2012009486A1	12 January 2012 (12-01-2012)
		US9083059B2	14 July 2015 (14-07-2015)
		US2015311566A1	29 October 2015 (29-10-2015)
		US9450273B2	20 September 2016 (20-09-2016)
		WO2010110159A1	30 September 2010 (30-09-2010)
US9455476B2	27 September 2016 (27-09-2016)	US2010196764A1	05 August 2010 (05-08-2010)
		US9455476B2	27 September 2016 (27-09-2016)
		CN101826631A	08 September 2010 (08-09-2010)
		EP2216844A2	11 August 2010 (11-08-2010)
		EP2216844A3	27 October 2010 (27-10-2010)
		JP2010182482A	19 August 2010 (19-08-2010)
		JP4992919B2	08 August 2012 (08-08-2012)